AD NUMBER
AD844919
LIMITATION CHANGES
TO: Approved for public release; distribution is unlimited.
FROM: Distribution authorized to U.S. Gov't. agencies and their contractors; Critical Technology; NOV 1968. Other requests shall be referred to Air Force Technical Applications Center, Washington, DC. This document contains export-controlled technical data.
AUTHORITY
usaf ltr, 25 jan 1972

AD844919

LARGE-ARRAY SIGNAL AND NOISE ANALYSIS

Special Scientific Report No. 25

LOCATION STATISTICS FOR FREQUENCY-WAVENUMBER PROCESSING

Prepared by

Wayne W. Wilkins   Leo N. Heiting

Frank H. Binder, Program Manager

TEXAS INSTRUMENTS INCORPORATED
Science Services Division
P.O. Box 5621
Dallas, Texas 75222

Contract No. AF 33(657)-16678

Prepared for

AIR FORCE TECHNICAL APPLICATIONS CENTER
Washington, D.C. 20333

Sponsored by

ADVANCED RESEARCH PROJECTS AGENCY
ARPA Order No. 599
AFTAC PROJECT No. VT/6707

DEC 19 1968

A

21 November 1968

LARGE-ARRAY SIGNAL AND NOISE ANALYSIS

Special Scientific Report No. 25

LOCATION STATISTICS FOR FREQUENCY-WAVENUMBER PROCESSING

Prepared by

Wayne W. Wilkins   Leo N. Heiting

Frank H. Binder, Program Manager

TEXAS INSTRUMENTS INCORPORATED
Science Services Division
P.O. Box 5621
Dallas, Texas 75222

Contract No. AF 33(657)-16678

AIR FORCE TECHNICAL APPLICATIONS CENTER
Washington, D.C. 20333

attn: Vela Seismological Center

Sponsored by

ADVANCED RESEARCH PROJECTS AGENCY
ARPA Order No. 599
AFTAC PROJECT No. VT/6707

21 November 1968

BLANK PAGE

ABSTRACT

Results of a computer study which theoretically determined the detection and location capabilities of various wavenumber spectra techniques are presented in this report. Two distinct short-period array configurations were simulated. The first configuration simulated was a 13-element array employing the outputs of the inner 13 subarrays of the Montana LASA. In this case, the ambient noise was considered to be completely uncorrelated. The second configuration simulated consisted of all or a portion of a standard LASA subarray. Various noise models, made up of mostly organized noise, were used. Four spectral techniques — the conventional spectrum, two high-resolution spectra, and the probabilistic processor — were evaluated. Unfortunately, an error in the program, which could not be rectified in time for inclusion of correct results in this report, prevented evaluating the detection capability of the probabilistic processor.

When wavenumber spectra at a single frequency are used to locate a signal in uncorrelated noise, all four techniques must yield exactly the same location. It was found that events with an SNR of 1.0 or greater were almost always located properly within the resolving power of the grid points at which the spectra were calculated. Wideband frequency-domain location can be accomplished by computing wavenumber spectra at several independent frequencies and summing the spectra in a velocity-preserving manner before choosing the peak-power location.

Conventional spectra of signals in uncorrelated noise were computed at five independent frequencies and summed. This procedure resulted in no incorrect locations for SNR's of 0.5 or greater, thereby indicating its significant superiority over the location ability of single-frequency spectra.

The wideband wavenumber spectral technique is roughly analogous to time-domain beamforming, and the results obtained here may be indicative of those achievable in the time domain.

The performance of the small arrays in organized noise was found to be markedly inferior to the performance of the large array using uncorrelated noise. The conventional spectrum seems to have no practical detection ability, while the high-resolution techniques are perhaps marginal in this respect. All techniques located a significant number of events improperly, even when the SNR was as high as 6.48.
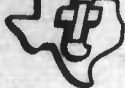
TABLE OF CONTENTS

APPENDIXES

ILLUSTRATIONS

science services division

ILLUSTRATIONS (CONT)

SECTION I

INTRODUCTION

The relationship between the detection or location of short-period seismic events using wavenumber spectra and the signal-to-noise ratio (SNR) of the data being processed was studied, and the results are presented in this report.

The need for an effective detection mechanism to monitor underground nuclear tests is obvious. Reasonably accurate location techniques assist in the classification problem, since events from many areas can be rejected immediately. More importantly, the approximate location of an event is required for effective off-line beamsteer or MCF processing performed to enhance classification parameters.

This study was initially undertaken analytically but soon became intractable. The problem was then divided into two experiments designed to determine empirically the location and detection abilities of particular array geometries as a function of SNR. The two tests treat correlated noise and uncorrelated noise separately and process correlated noise at the subarray level and uncorrelated noise using LASA A-, B-, C-, and D-ring subarrays. This separation into two experiments results from the increased computational difficulty in contrasting correlated noise to uncorrelated noise. Both data generation and processing techniques require matrix rather than vector arithmetic when the noise field is correlated.

For each of the two experiments, four techniques were evaluated, with all processing in the frequency-wavenumber domain. The techniques are the conventional wavenumber spectrum, the probabilistic processor, and two forms of high-resolution wavenumber spectra. Both forms of high-resolution wavenumber spectra were found to have equivalent averaged properties for a uniform plane-wave signal and normalized $\vec{f}\text{-}\vec{k}$ spectra; therefore, this report usually reflects the averaged properties of both techniques.
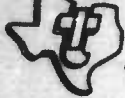
For the processing, a random-number generator generates a sequence of normal (mean = 0, variance = 1) random numbers which are paired and grouped to form a set of 100 random complex vectors. The set of vectors is transformed to a second set of random complex vectors having a specified covariance matrix. The latter vectors are taken to be noise transform vectors with the specified noise crosspower matrix. A scaled signal transform vector is added to each noise transform vector to form the data transform vector. The signal is scaled to yield a desired signal-to-noise power ratio. Resulting data are then processed by each of the processors at selected points in the vicinity of the signal location in K-space. In the correlated noise cases, the values obtained for each noise vector over K-space are normalized to have a unit sum. The mean and standard deviation at each wavenumber point for each processor are the outputs of the computer program. The program steps may be repeated using the same signal and noise vectors but with a different signal scale factor. An error was detected in the program which generates this output for the probabilistic processor. Since time did not permit correction of the error, the means and standard deviations are shown only for the conventional and high-resolution schemes.

The above steps yield mean wavenumber spectra for each of the four processing techniques at various signal-to-noise ratios and various noise models. From these results, it is possible to observe the mean behavior of a detection scheme as a function of SNR for the various types of noise fields.

A second type of output was also generated. For each of the 100 signal-plus-noise vectors, the location of peak power in K-space is determined. These results are then plotted, showing the number of times out of 100 that the peak power occurs at various K-space locations. This type of display provides an indication of the confidence that can be attached to the peak-power location for various SNR's.

science services division

SECTION II

PROCEDURES

A. PROCESSING EQUATIONS

The four schemes and the corresponding processing quantities evaluated are

- Conventional Wavenumber Spectrum (CS)

$$V^{*T} XX^{*T} V$$

- Probabilistic Processor (PP)

$$\frac{\dfrac{1}{|N + VV^{*T}|} \exp \left\{ X^{*T} \left[N + VV^{*T} \right]^{-1} X \right\}}{\sum_{k} \dfrac{1}{|N + VV^{*T}|} \exp \left\{ -X^{*T} \left[N + VV^{*T} \right]^{1} X \right\}}$$

- High-Resolution Wavenumber Spectrum (HR1)

$$\frac{\delta}{V^{*T} V - \dfrac{1}{\delta + X^{*T} X} \, V^{*T} XX^{*T} V}$$

- High-Resolution Wavenumber Spectrum (HR2)

$$\frac{\delta^{2}}{V^{*T} V - \dfrac{2\delta + X^{*T} X}{(\delta + X^{*T} X)^{2}} \, V^{*T} XX^{*T} V}$$

In these equations,

N is the noise covariance matrix

X is the vector of data transforms

science services division

$V = V(k)$ is the vector of phase shifts appropriate for the frequency and velocity of a plane wave propagating across the array

$| \; |$ denotes the determinant of the enclosed matrix

δ is a scalar

$*$ is conjugate

T is transpose

Brief derivations of the probabilistic processor and high-resolution equations are given in Appendix A. Appendix B provides an efficient method for evaluation of $|N + VV^{*T}|$.

For the case in which the noise is uncorrelated, the covariance matrix N is the identity matrix I, and the data manipulations reduce to vector arithmetic for both data generation and data processing. Appendix B shows that

$$|N + VV^{*T}| = |N|(1 + S^{*T}V^{*T}VS)$$

where

$$SNS^{*T} = I$$

$$I = \text{identity matrix}$$

For $N = I$, the determinant simply becomes $1 + M$, where M is the number of channels.

The quadratic form in the PP equation may be written as

$$X^{*T}\left[N + VV^{*T}\right]^{-1}X = X^{*T}N^{-1}X - \frac{X^{*T}N^{-1}VV^{*T}N^{-1}V}{1 + V^{*T}N^{-1}V}$$

For N = I, this reduces to

$$X^{*T}X - \frac{X^{*T}VV^{*T}X}{1 + V^{*T}V}$$

The term $X^{*T}X$ is the sum of the power in each channel at the frequency being processed, and $V^{*T}V = M$, the number of channels. Thus, using uncorrelated noise, the quadratic forms of the high-resolution schemes and the probabilistic processor scheme are different combinations of the conventional wavenumber spectrum, the sum of the power in each channel and the number of channels. All four techniques have their peak values at the same wavenumber location. Using correlated noise, the probabilistic processor does not necessarily have its peak at the same location as the other three schemes.

B. DATA GENERATION

Let N denote a noise crosspower matrix. It is desired to generate a sequence of random complex vectors $Z_i^T = \left(Z_{i1}, Z_{i2}, \ldots, Z_{im}\right)$ having the covariance matrix N. Let $\{Y\}$ denote a set of complex vectors satisfying

$$EY_i = 0$$

$$EY_i Y_i^{*T} = I$$

where E is the expected value. There exists a matrix S such that

$$N = SS^{*T}$$

Then Z_i is generated by

$$Z_i = SY_i$$

Note that

$$EZ_i = ESY_i$$

$$= SEY_i$$

$$= 0$$

and

$$EZ_i Z_i^{*T} = ESY_i Y_i^{*T} S^{*T}$$

$$= SEY_i Y_i^{*T} S^{*T}$$

$$= SIS^{*T}$$

$$= N$$

Let s be a unit plane-wave signal transform vector and form the vector X_i by

$$X_i = Z_i + \alpha s$$

where α is a scale factor. The vector X_i is then the data transform vector.

C. UNCORRELATED NOISE PROCESSING

In the experiment using uncorrelated noise, each processor used data having an infinite velocity signal from 13 channels of the LASA A-, B-, C-, and D-ring subarray locations. Figures II-1 and II-2 show the mean and standard deviation of the processor outputs as a function of wavenumber for SNR's of 0.72 and 1.12. These statistics were estimated at 11 equally spaced points along the N-S axis from the origin to k (wavenumber) = 0.1 cycle/km. Figure II-3 gives the mean and standard deviation as a function of SNR.

In addition to calculating the mean and standard deviation, each of the 100 signal-plus-noise vectors was processed to determine the peak-power location. As mentioned previously, each of the four techniques leads to the same location.

Figure II-4 gives the relative frequency of occurrence of peak power at 25 wavenumber locations equispaced along the N-S axis between the origin and 0.096 cycle/km. These computations are performed at a single frequency for three different values of SNR. Smoothing can be achieved by computing wavenumber spectra at several independent frequencies within the range where the peak SNR occurs. A velocity-preserving stack of the individual spectra is then formed before choosing the peak-power location. This procedure with conventional spectra is analagous to forming time-domain beams for the various wavenumber locations and choosing the largest beam-steer output.

Figure II-5 shows the relative frequency of occurrence after stacking over five frequencies. The time gate used in obtaining transforms from real data must be short in order to contain only that portion of the record where the signal is largest but must be long enough to provide reasonable crosspower estimates for the widely spaced seismometers. For short-period processing out to the LASA D-ring, about 15 sec is a good compromise. From sampling theory, this results in an independent frequency increment of $1/15 = 0.067$ Hz. Thus, by smoothing wavenumber spectra over five adjacent independent frequencies, an effective band of 0.33 Hz is covered.

D. CORRELATED NOISE PROCESSING

Three general types of noise fields were generated:

- An isotropic disk centered at the origin
  with a radius of 0.1 cycle/km and having
  20 percent uncorrelated noise added.

- An isotropic disk centered at $k = 0.05$
  (on N-S axis) with a radius of 0.01 cycle/
  km and having 1-percent uncorrelated
  noise added

- Istropic disks centered at $k = 0.05$ (on
  N-S axis) with a radius of 0.025 cycle/
  km and having 1-percent, 10-percent,
  and 20-percent uncorrelated noise added

The first two models used a standard LASA subarray and had
25 channels of data. The last model used the center and outer 15 locations
of a standard LASA subarray and had 16 channels of data. All processing used
an infinite-velocity signal. The equations were evaluated at 11 equally spaced
points on the N-S axis from the origin to $k = 0.1$ cycle/km. Signal-to-noise
ratios ranged from about 0.0004 to 0.8. Again, the three types of displays
shown in Figures II-6 through II-20 are mean and standard deviation vs wave-
number, mean and standard deviation vs SNR, and relative frequency of
occurrence of peak power.
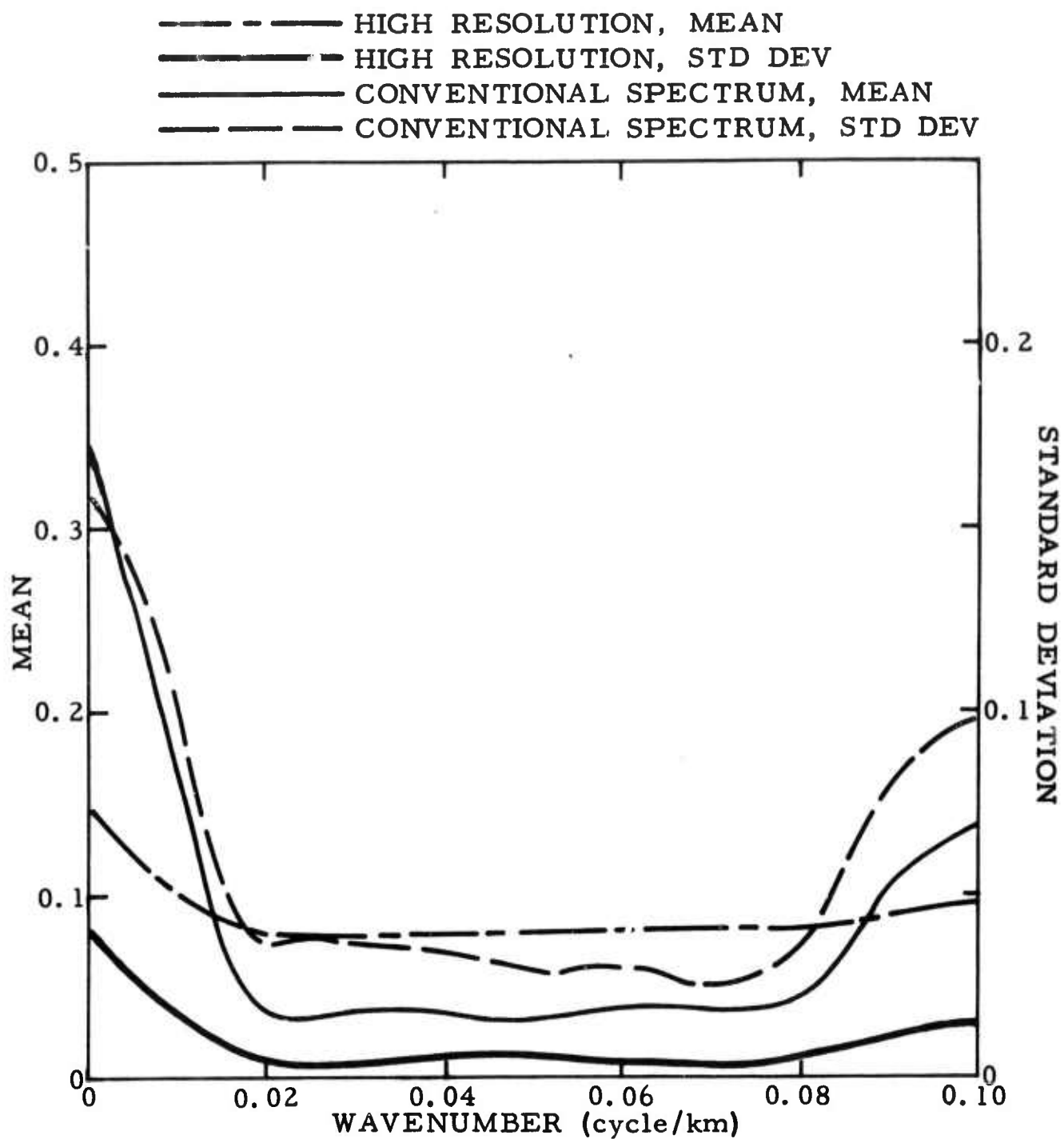
Figure II-1.   Mean and Standard Deviation Vs k, Uncorrelated Noise, SNR = 0. 72

science services division
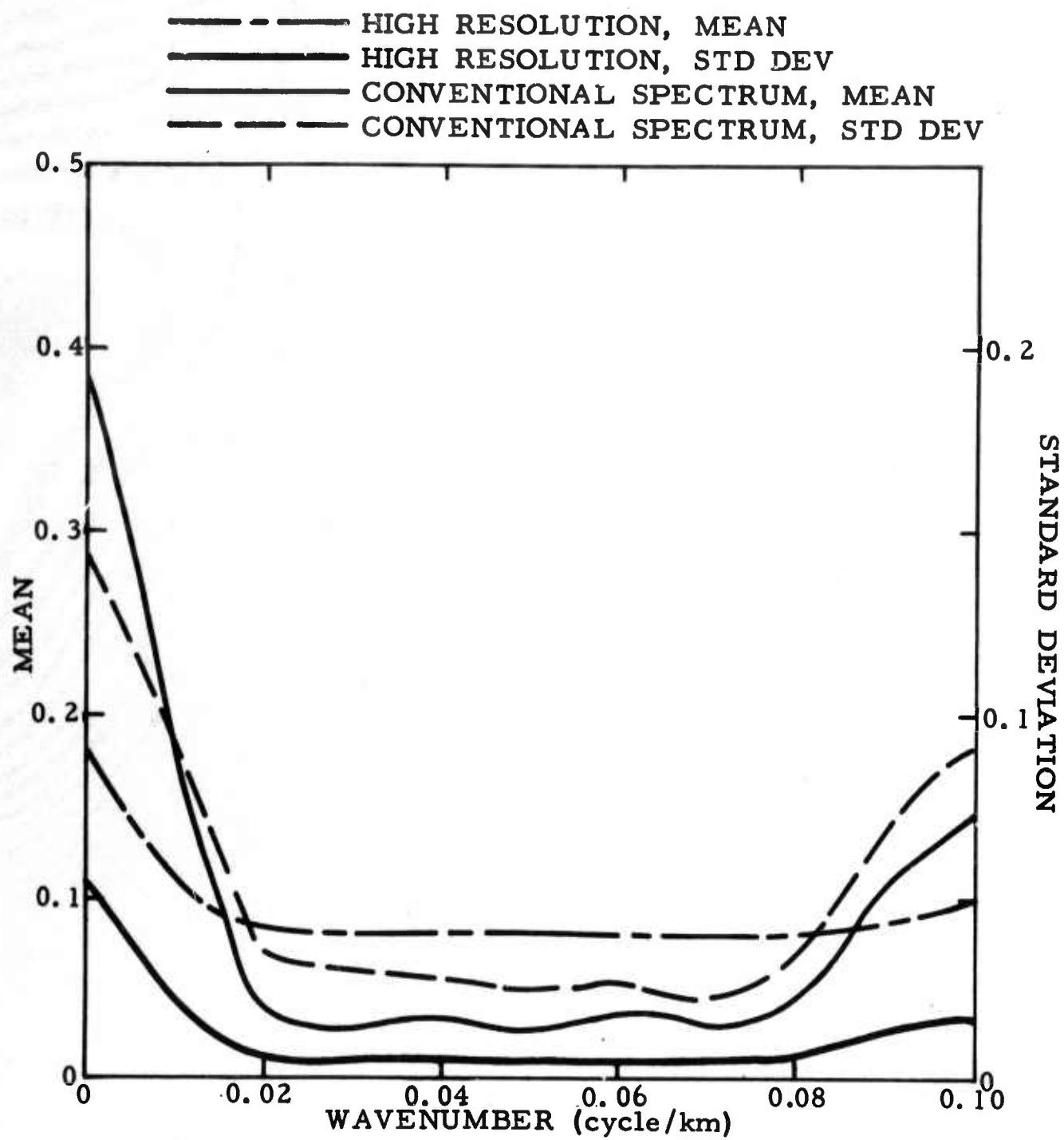
Figure II-2.   Mean and Standard Deviation Vs k, Uncorrelated Noise, SNR = 1. 12

science services division
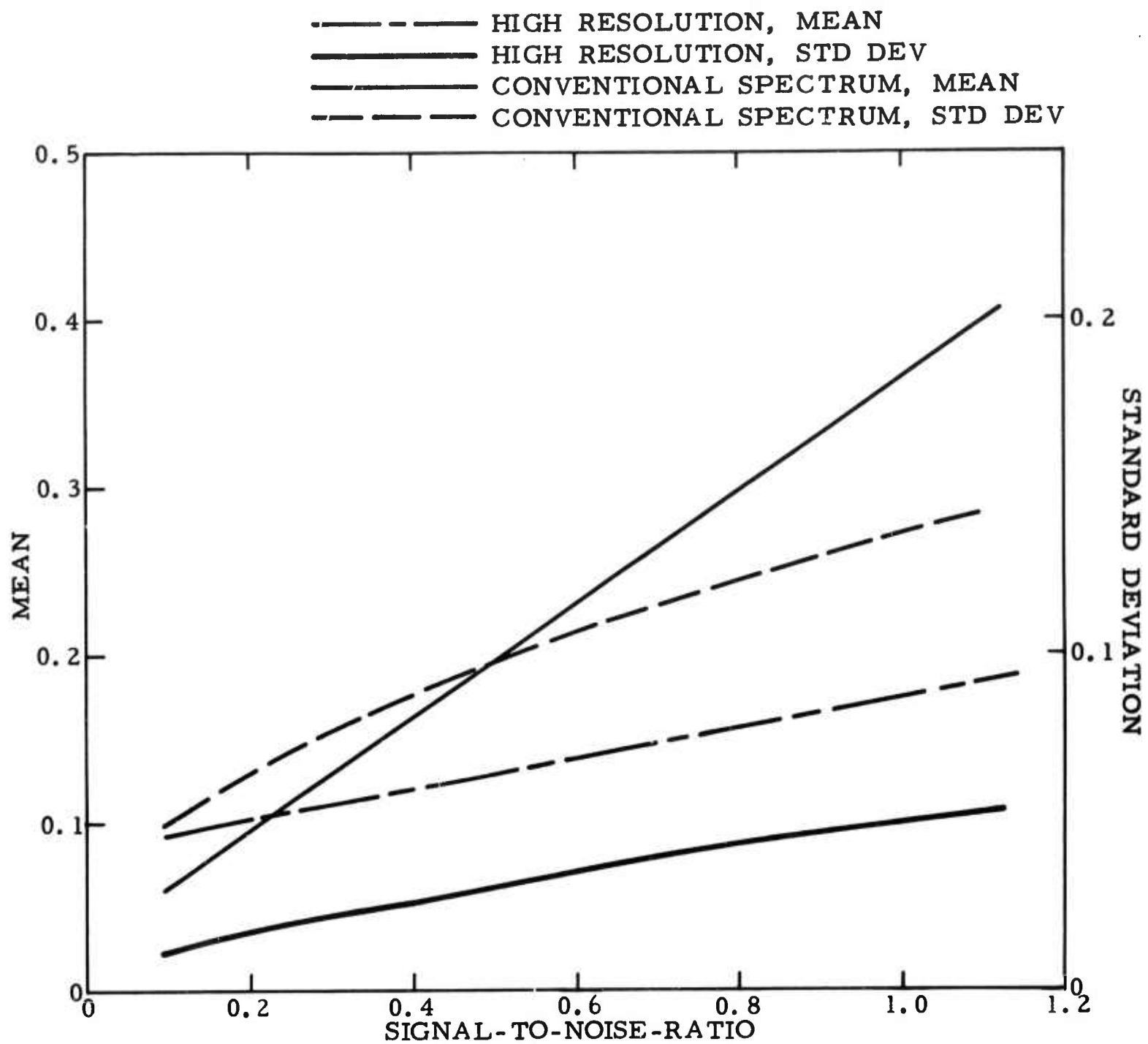
Figure II-3. Mean and Standard Deviation Vs SNR at k = 0.0 cycle/km, Uncorrelated Noise
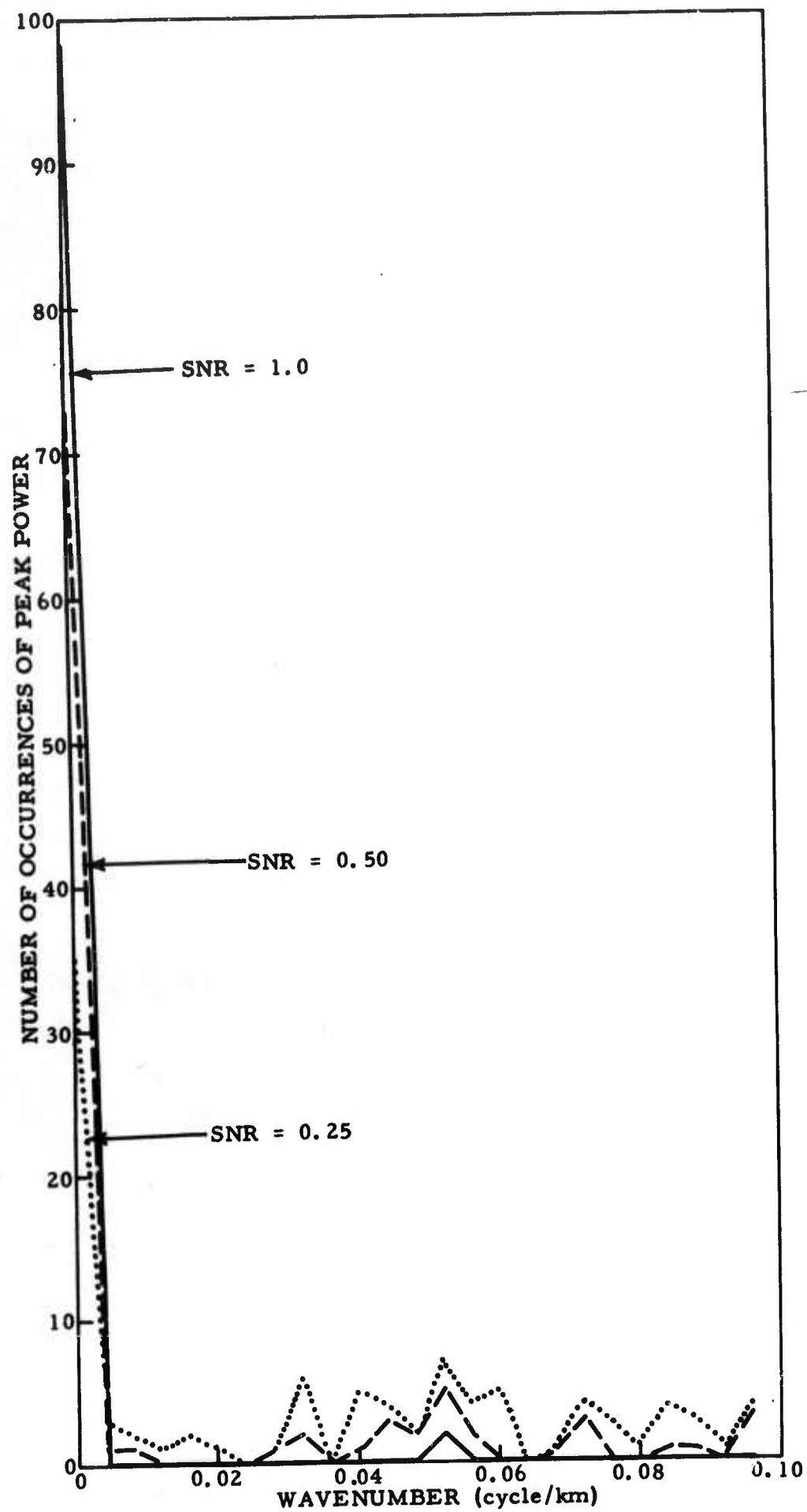
Figure II-4.   Distribution of Peak-Power Locations, Uncorrelated Noise

science services division
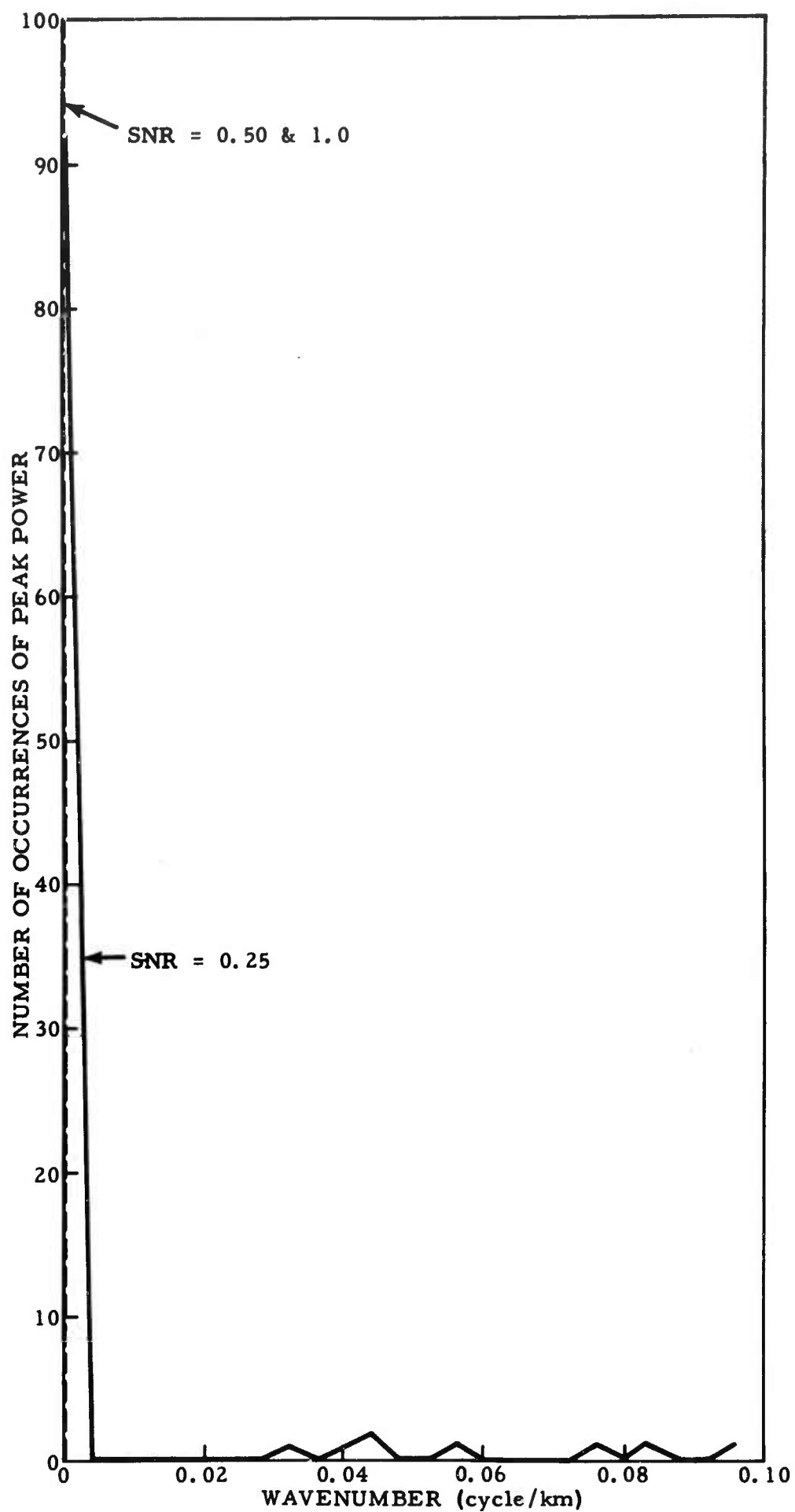
Figure II-5.   Distribution of Peak-Power Locations for Stacks
of Conventional Spectra, Uncorrelated Noise
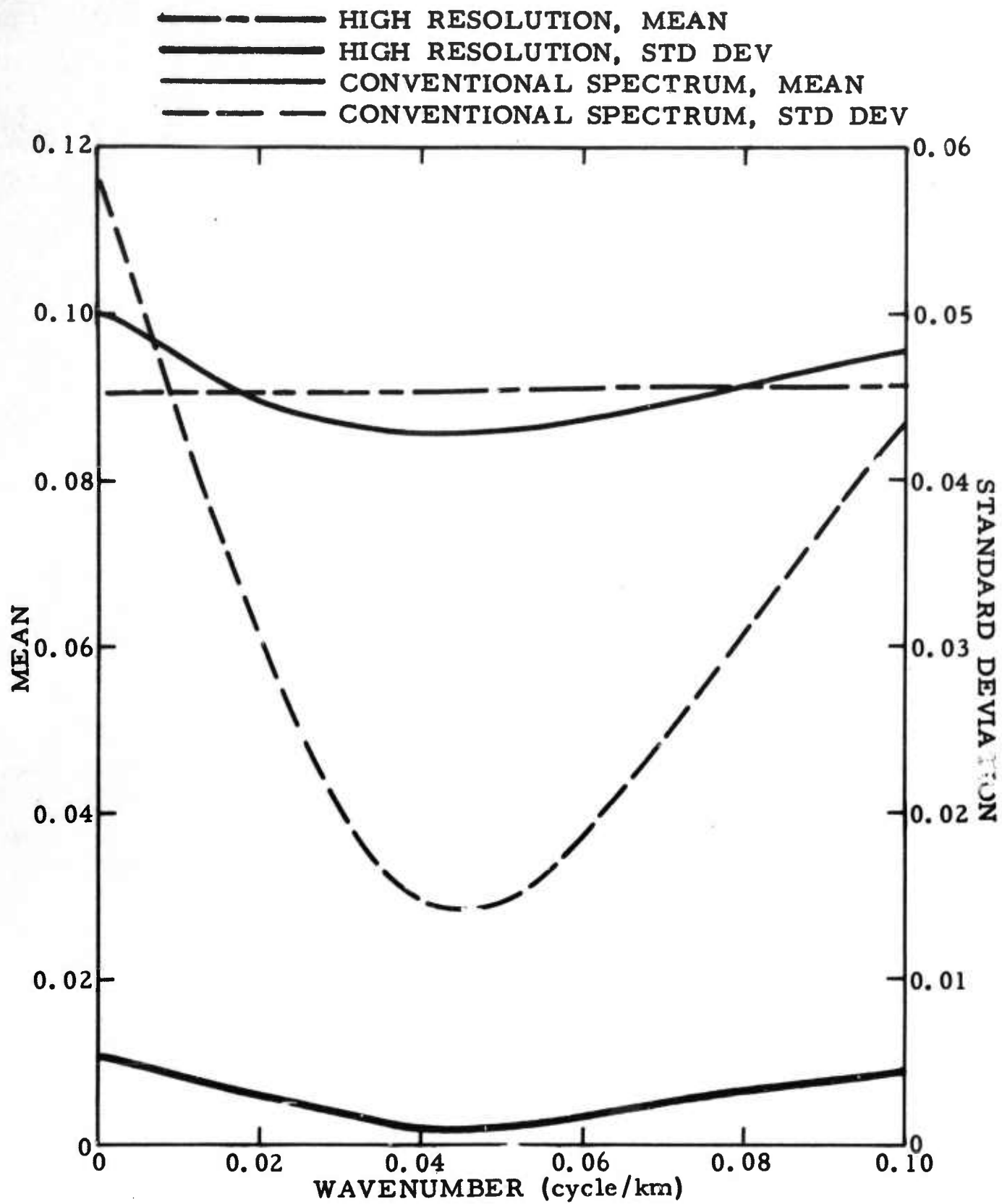
Figure II-6. Mean and Standard Deviation Vs k, Isotropic Bodywave Noise with 20-Percent Uncorrelated Noise Added, SNR = 0.0

science services division
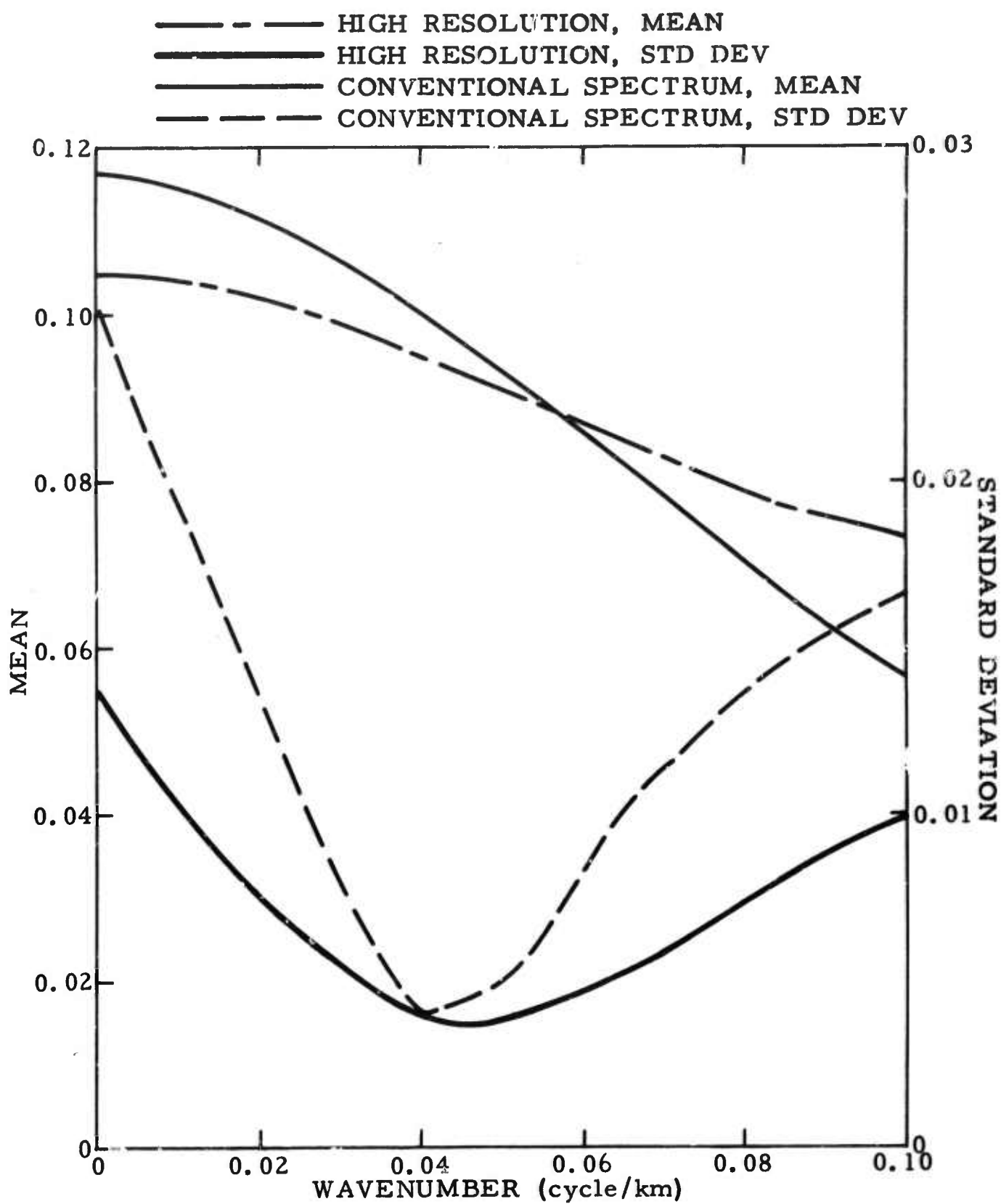
Figure II-7. Mean and Standard Deviation Vs k, Isotropic Bodywave Noise
with 20-Percent Uncorrelated Noise Added, SNR = 0.60

science services division
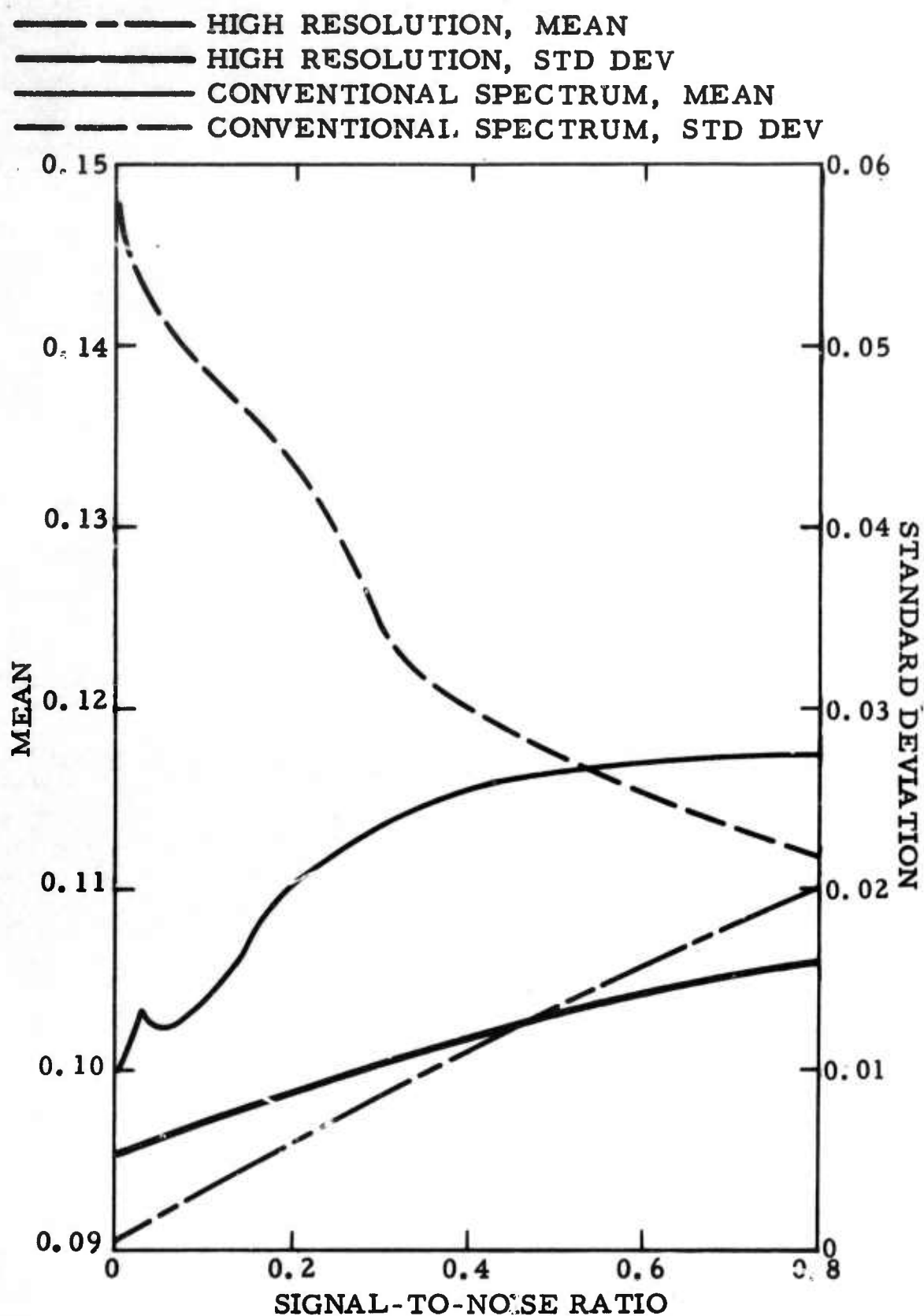
Figure II-8. Mean and Standard Deviation Vs SNR at k = 0.0 cycle/km, Iso-
tropic Bodywave Noise with 20-Percent Uncorrelated Noise Added

science services division
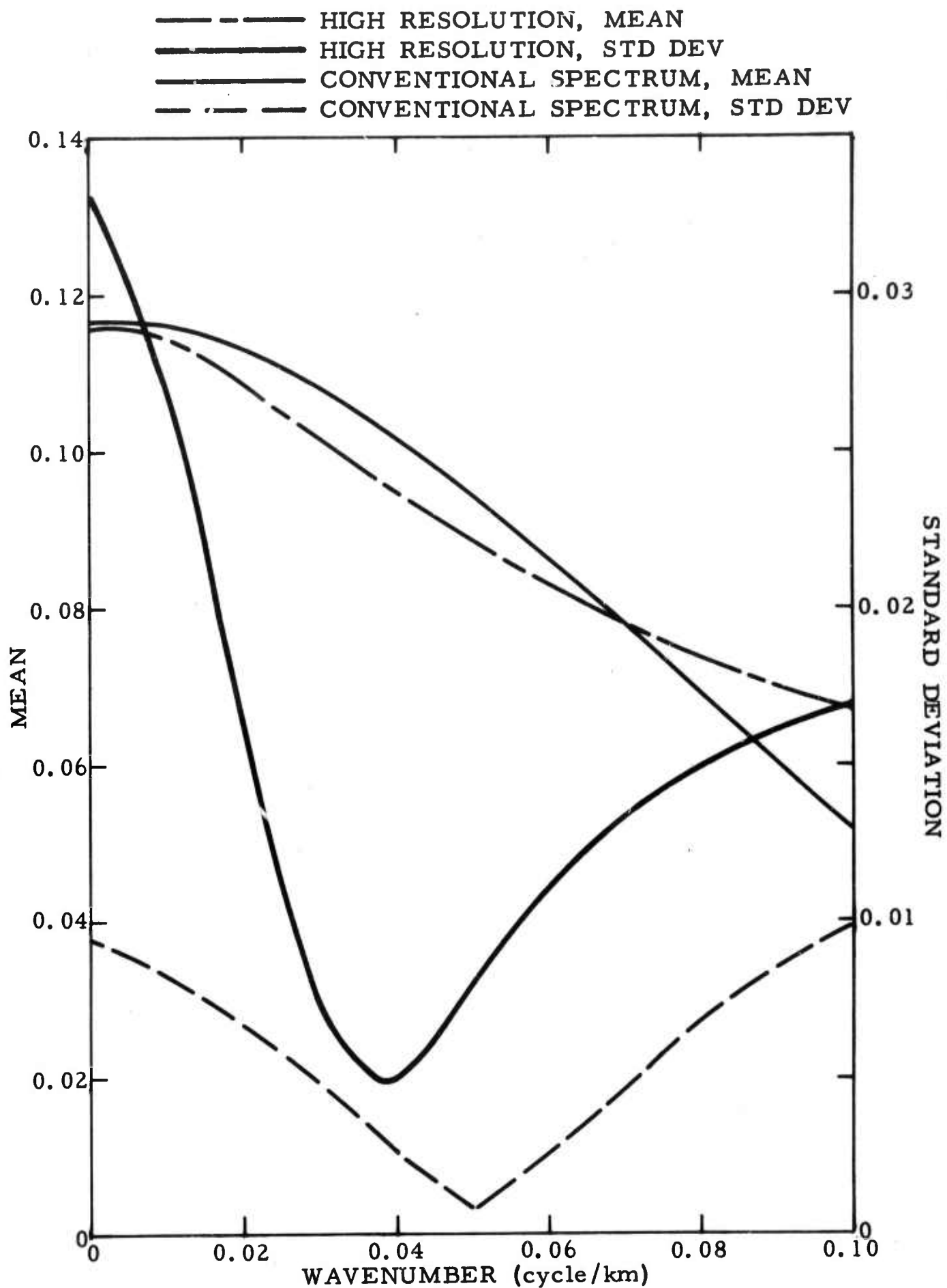
Figure II-9. Mean and Standard Deviation Vs k, Concentrated Directional
Noise with 1-Percent Uncorrelated Noise Added, SNR = 0.60
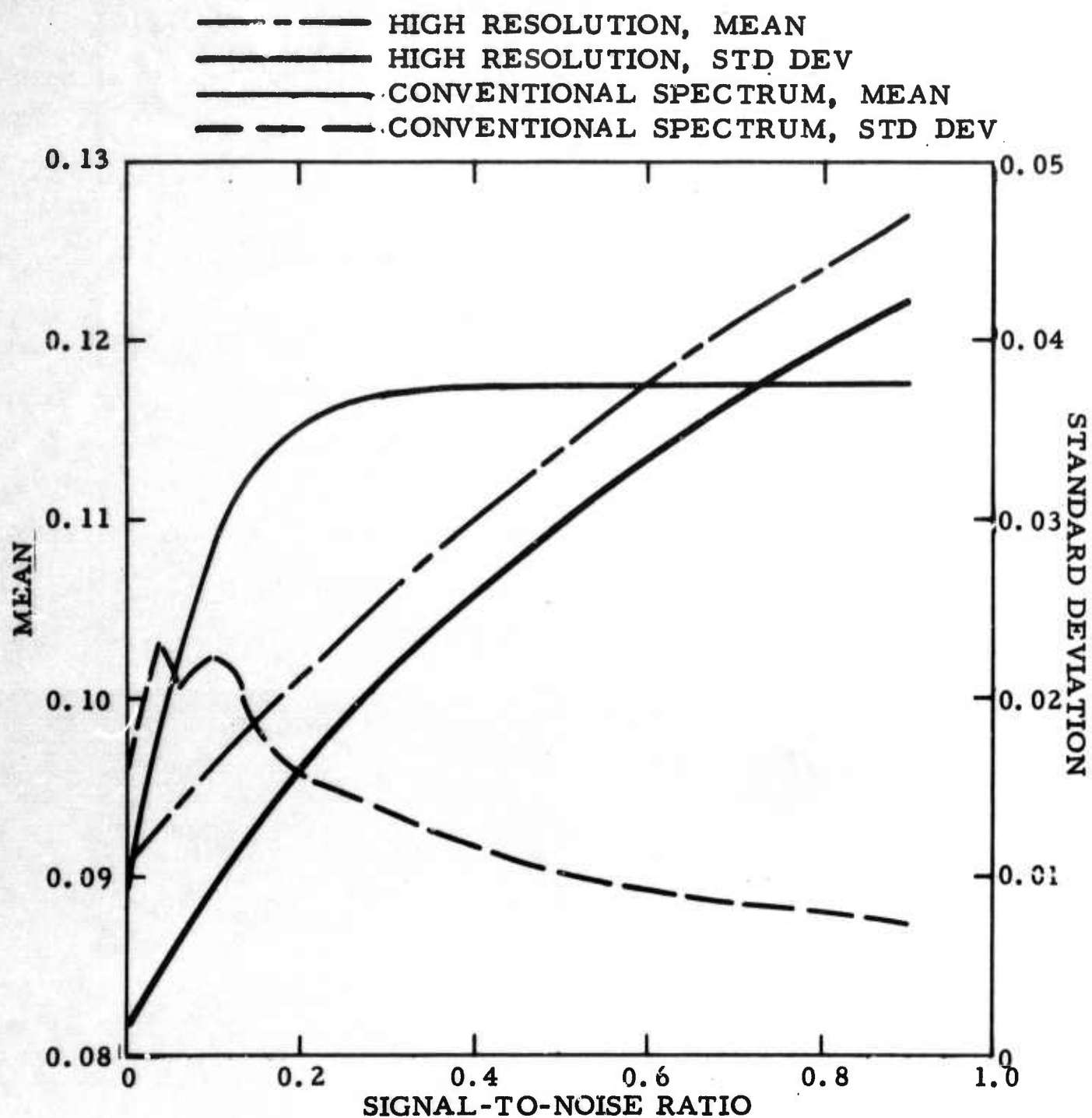
Figure II-10. Mean and Standard Deviation Vs SNR at k = 0.0 cycle/km, Concentrated Directional Noise with 1-Percent Uncorrelated Noise Added
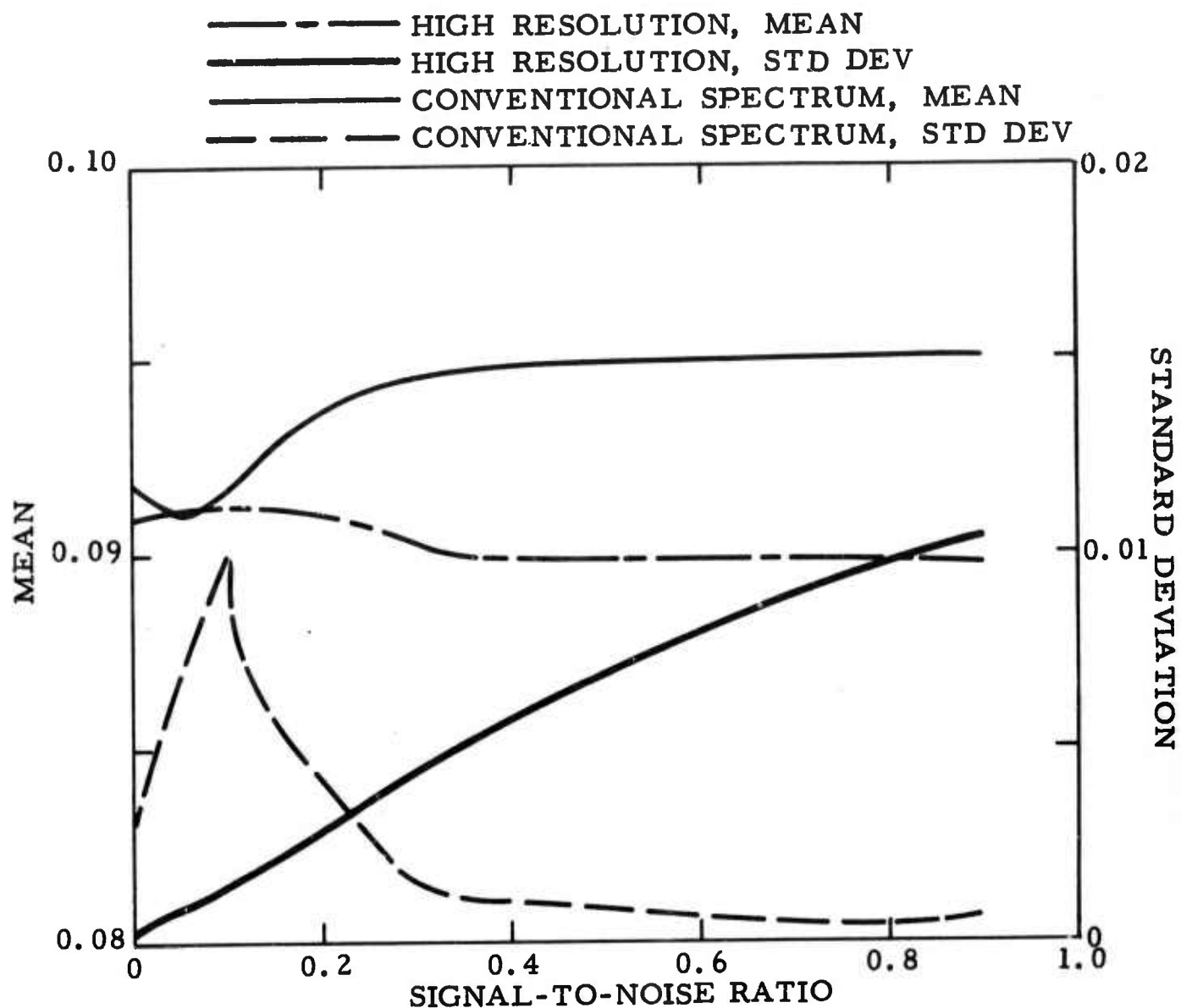
Figure II-11. Mean and Standard Deviation Vs SNR at k = 0.05 cycle/km, Concentrated Directional Noise with 1-Percent Uncorrelated Noise Added

science services division
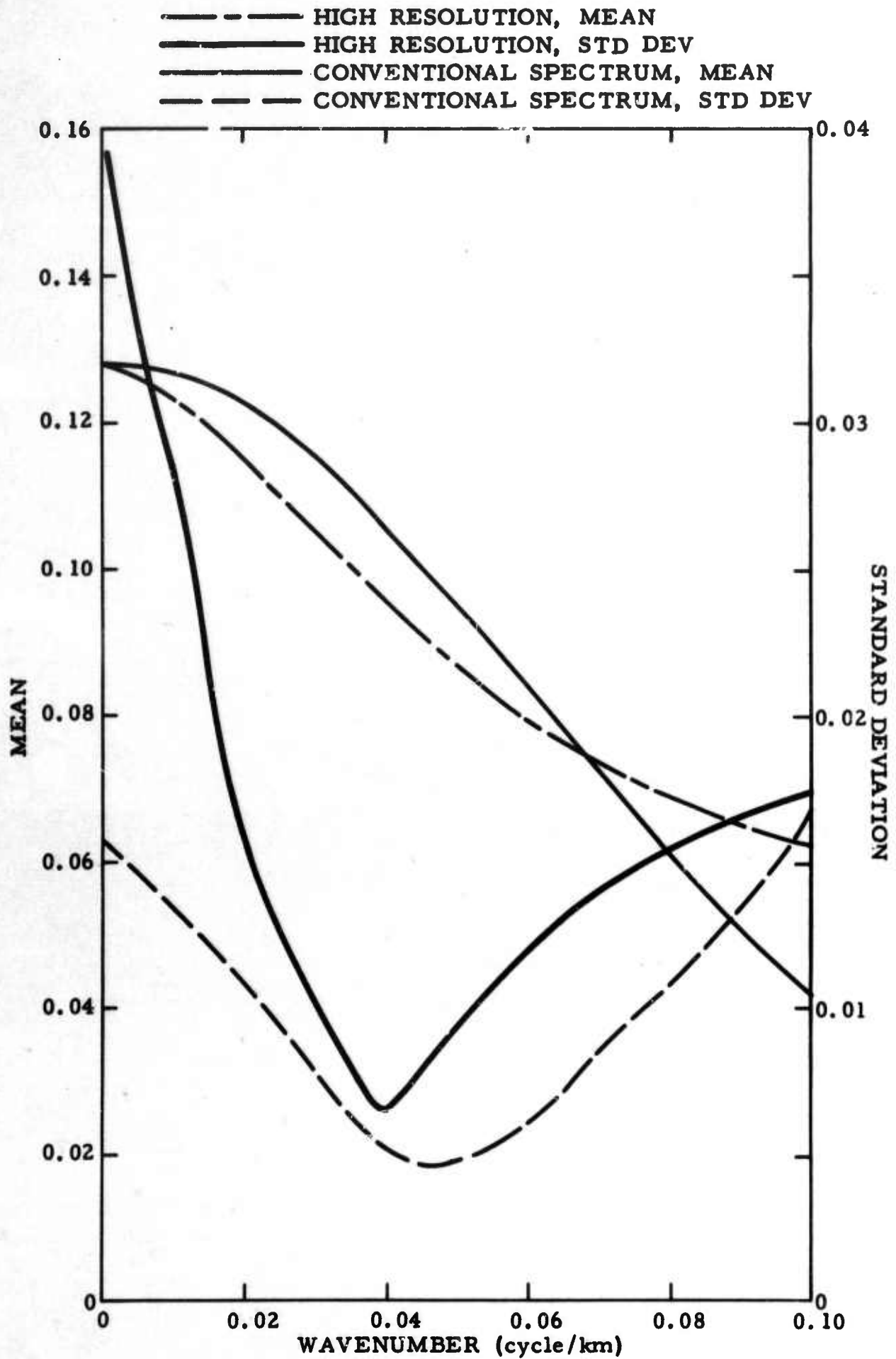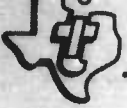
Figure II-12. Mean and Standard Deviation Vs k, Directional Noise with 1-Percent Uncorrelated Noise Added, SNR = 0.60
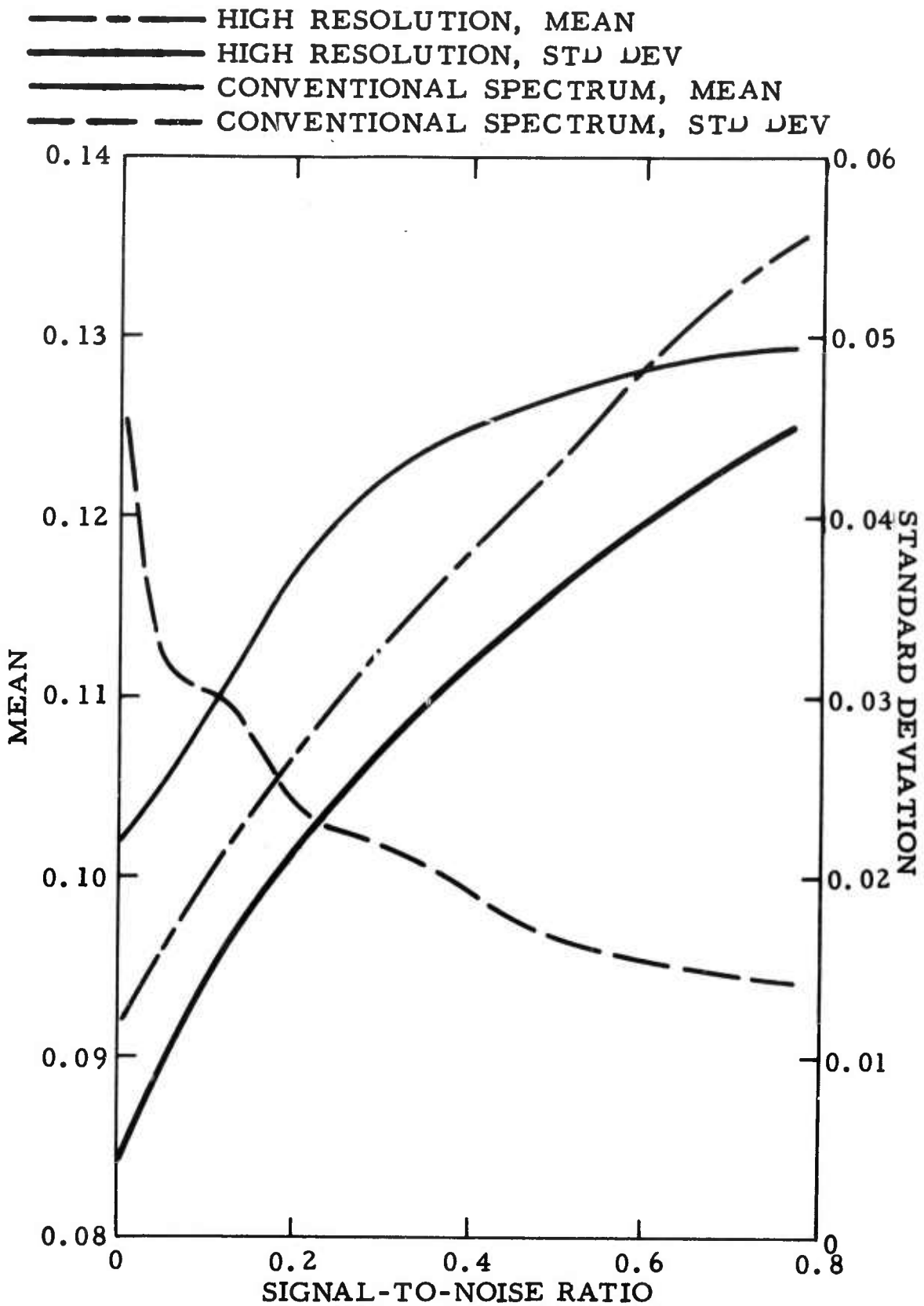
Figure II-13. Mean and Standard Deviation Vs SNR at k = 0. 0 cycle/km, Directional Noise with 1- Percent Uncorrelated Noise Added

science services division
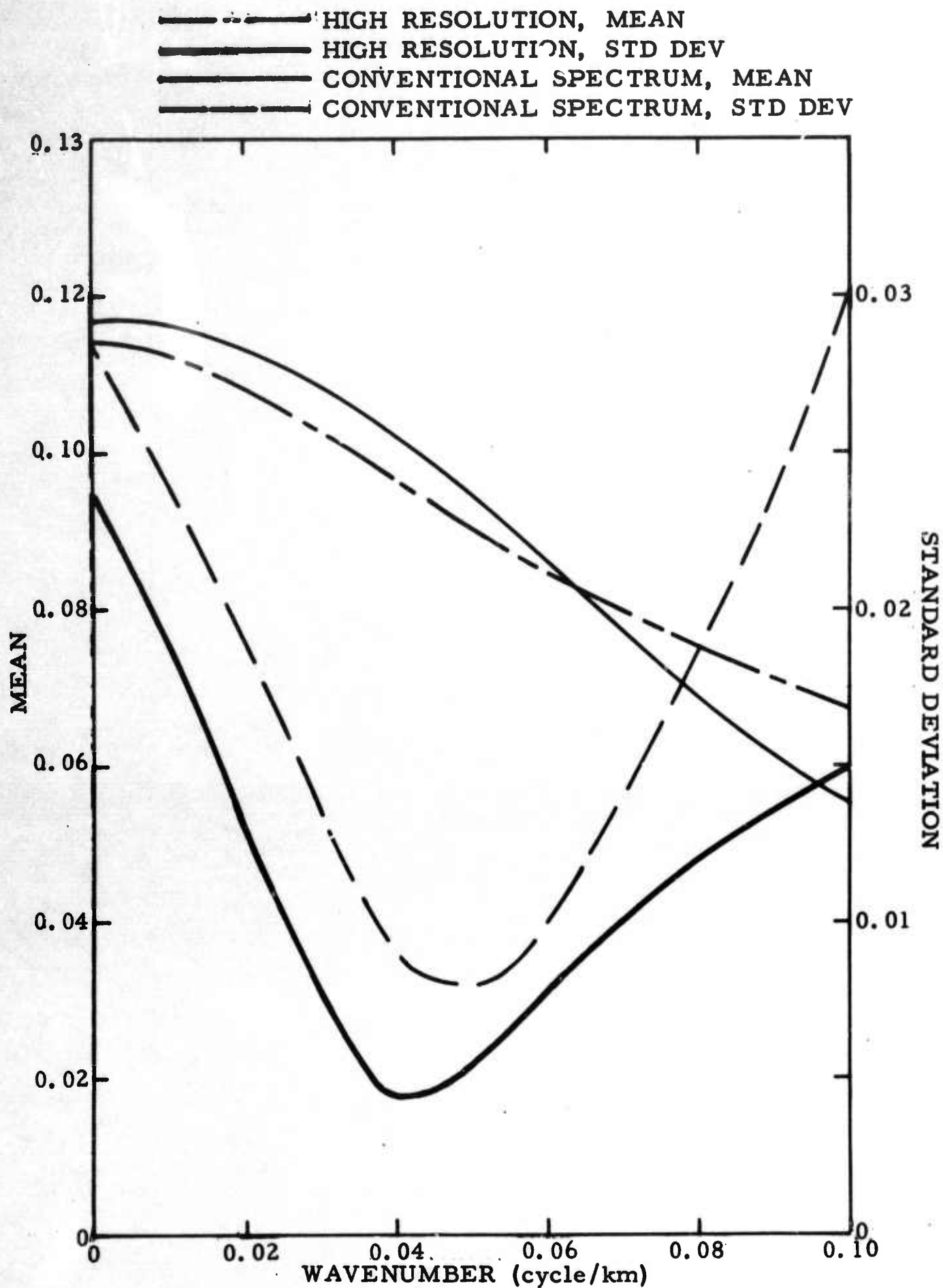
Figure II-14. Mean and Standard Deviation Vs k, Directional Noise with 10-Percent Uncorrelated Noise Added, SNR = 0.41
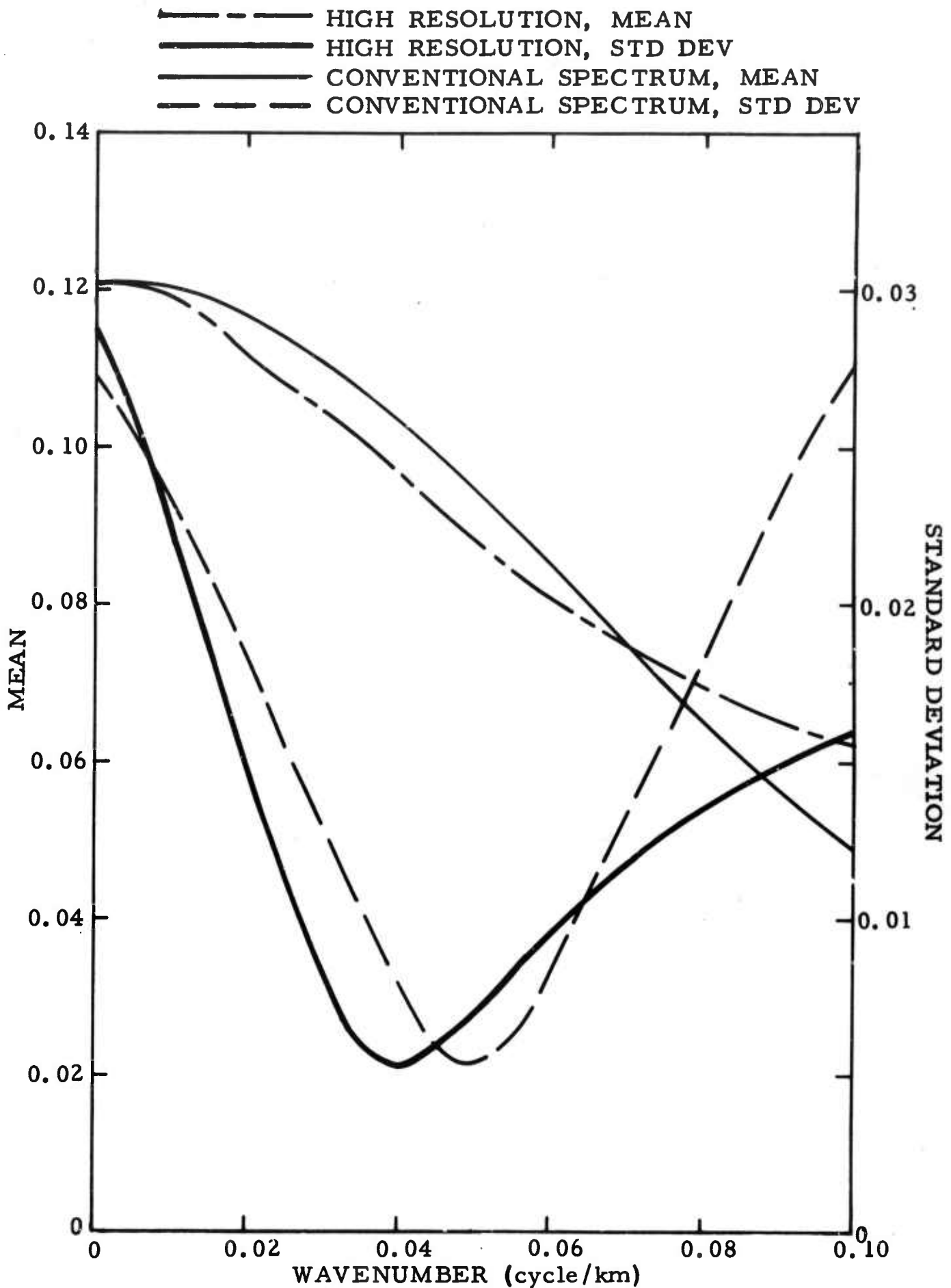
Figure II-15. Mean and Standard Deviation Vs k, Directional Noise with 10-
Percent Uncorrelated Noise Added, SNR = 0.60

science services division
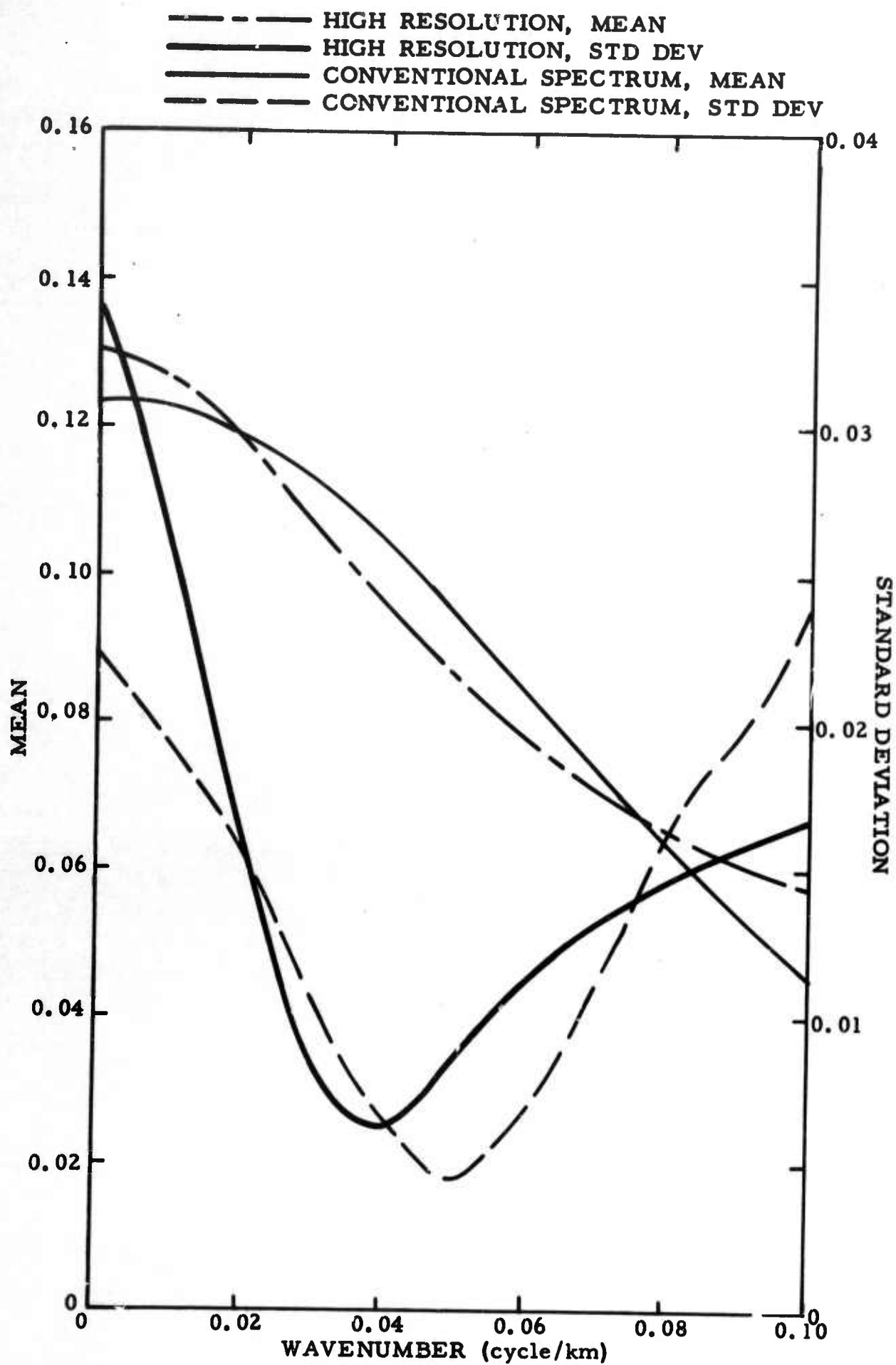
Figure II-16. Mean and Standard Deviation Vs k, Directional Noise with 10-Percent Uncorrelated Noise Added, SNR = 0.83

science services division
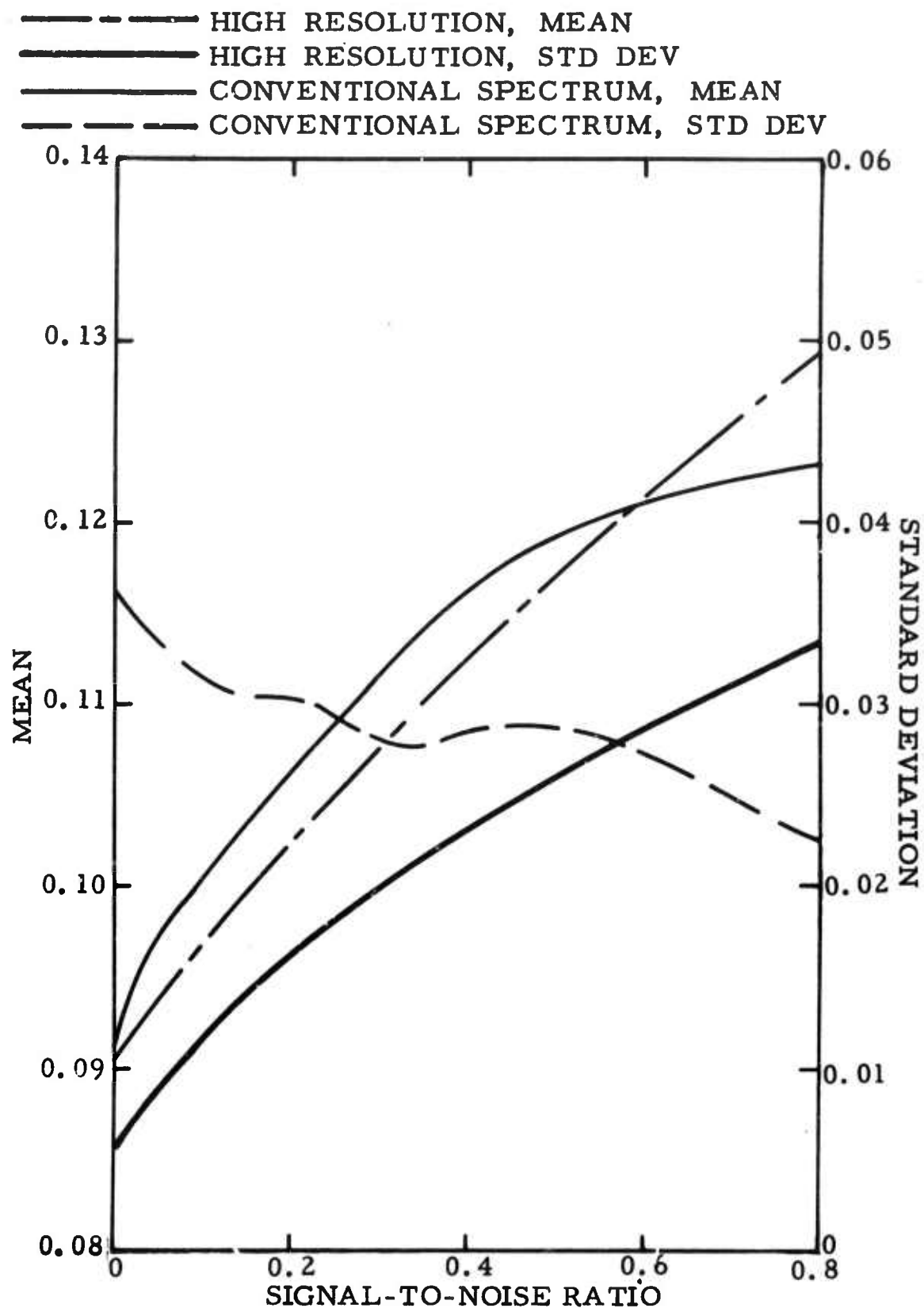
Figure II-17. Mean and Standard Deviation Vs SNR at k = 0. 0 cycle/km, Direc-
tional Noise with 10-Percent Uncorrelated Noise Added
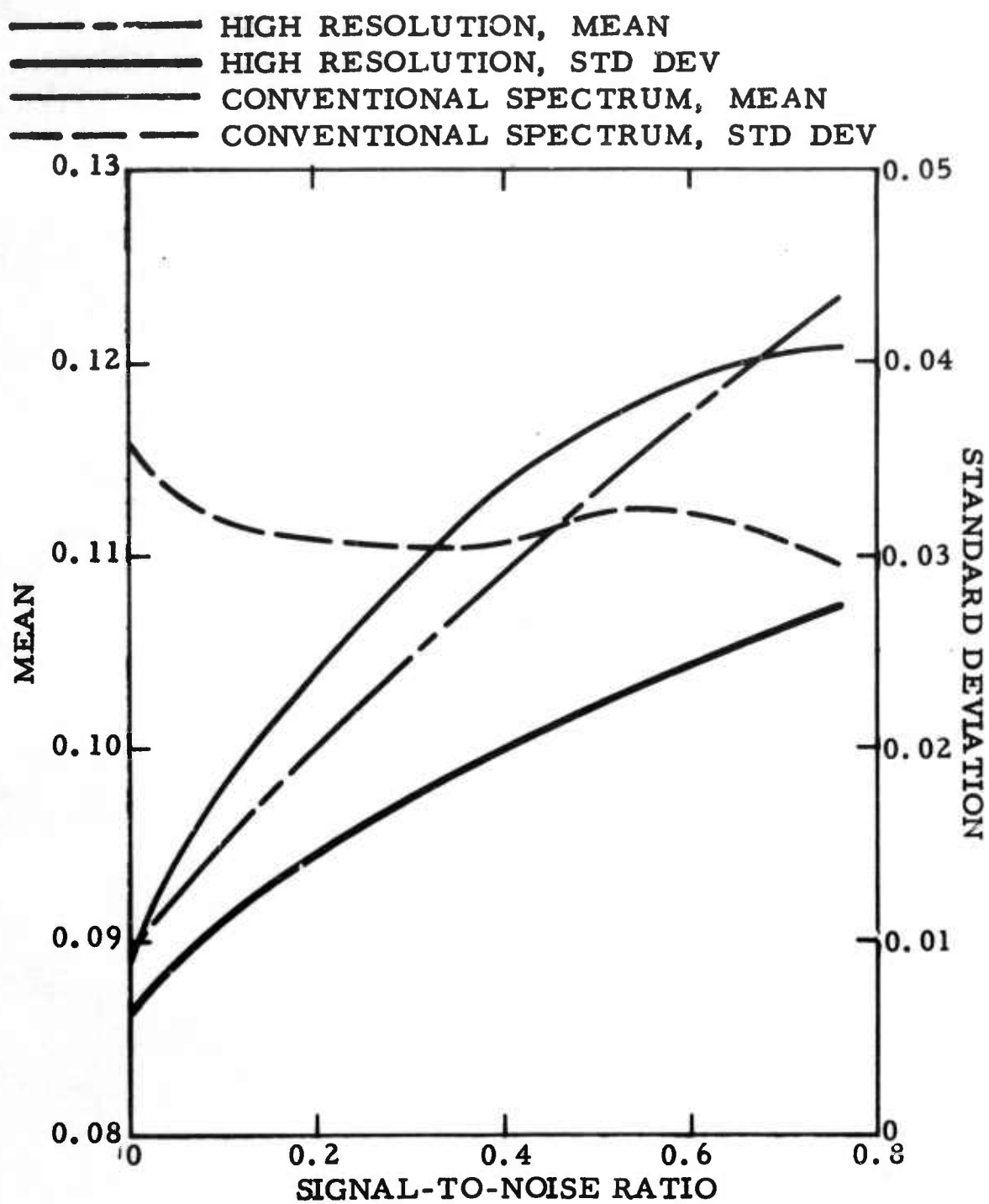
Figure II-18. Mean and Standard Deviation Vs SNR at k = 0.0 cycle/km, Directional Noise with 20-Percent Uncorrelated Noise Added
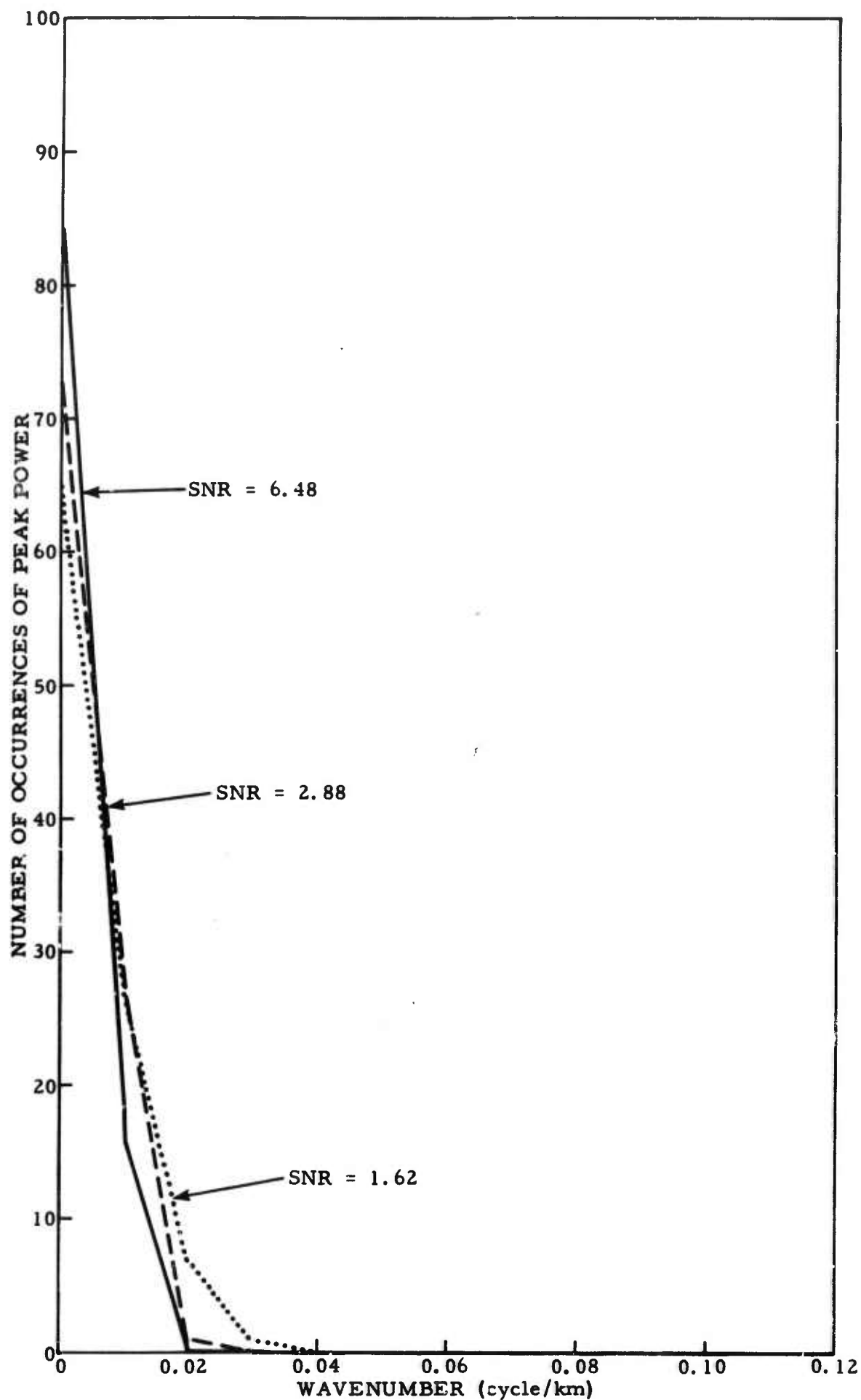
Figure II-19. Distribution of Peak-Power Locations for Conventional or High-Resolution Spectra, Directional Noise with 10-Percent Uncorrelated Noise Added

science services division
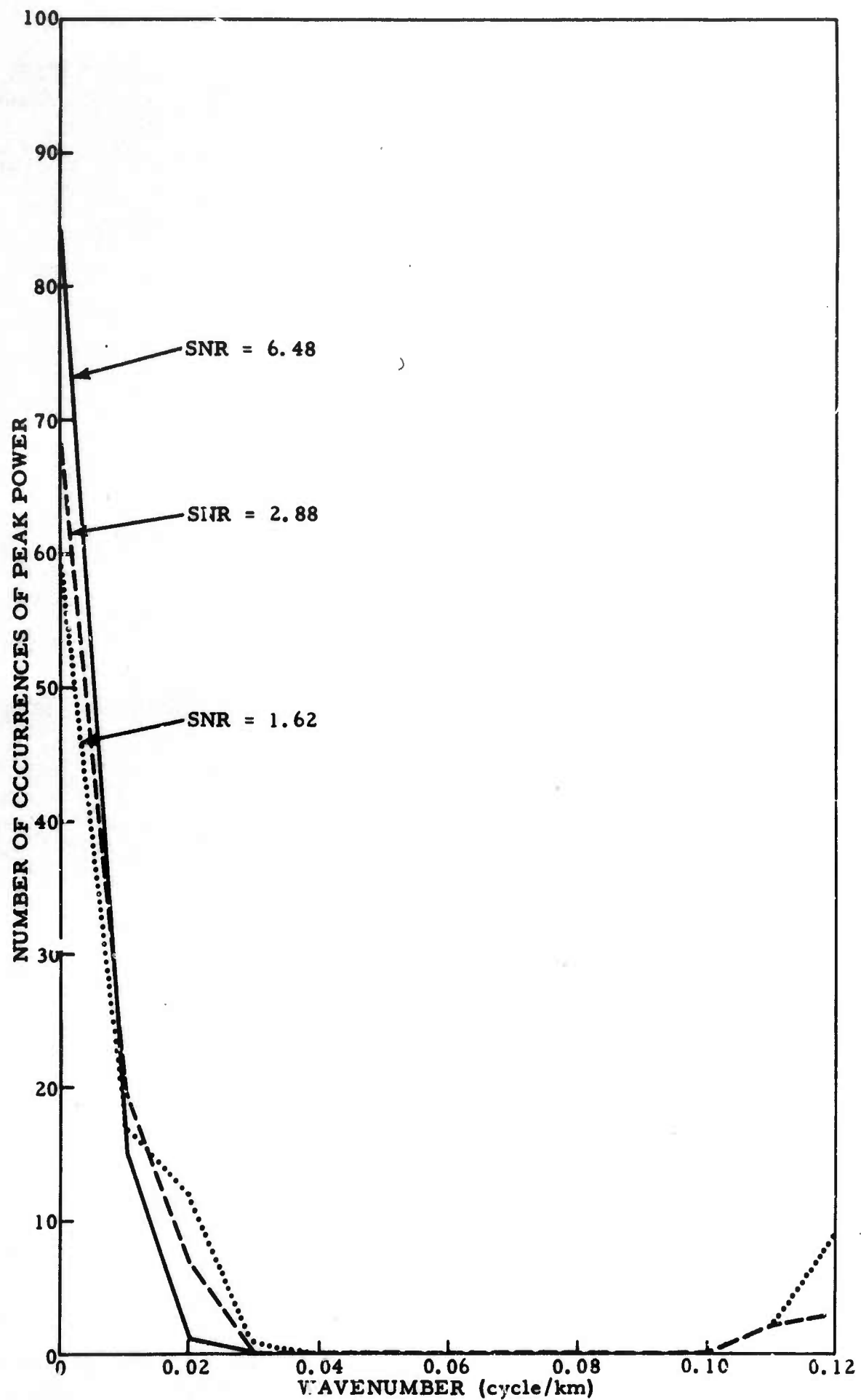
Figure II-20. Distribution of Peak-Power Locations for Probabilistic Processor, Directional Noise with 10-Percent Uncorrelated Noise Added

SECTION III
INTERPRETATION OF RESULTS

In all work discussed in this report, the signal was considered to have infinite velocity. Figures II-1 through II-5 show results obtained using the 13-element array conposed of the inner 13 subarray sites of the Montana LASA and a noise model consisting of completely uncorrelated noise.

Data presented in Figures II-1, II-2, and II-3 are useful in evaluating the relative merits of the conventional and high-resolution schemes for detection. Here, the problem is to select a threshold level which will almost always be higher than the largest peaks resulting from the ambient noise. The question is how large the SNR must be to assure that the signal peak will exceed the threshold.

Note that arbitrary scale factors were applied to the quantities plotted in these three figures, thereby resulting in apparent inconsistencies between the figures. The quantities displayed vary by orders of magnitude, and scaling was necessary to produce meaningful figures. Since the important quantity is the relationship between the mean and the standard deviation for a given processing scheme, the same scale factor was applied to these two measures.

Figures II-1 and II-2 show that the mean and standard deviation for both schemes have local maxima near 0.10 cycle/km; the spectral window of the array happens to have a peak in this region. Between 0.02 and 0.08 cycle/km, the means and standard deviations are quite constant. Moreover, the levels in this region are almost exactly the same as those observed at all wavenumbers in the absence of signal. Thus, the values of the mean and standard deviation at 0.04 cycle/km can be used as measures of the behavior of these techniques when uncorrelated noise alone is present.

In Figure II-2, the mean and standard deviation for the conventional spectrum at 0.04 cycle/km are 0.03 and 0.025, respectively. If a threshold two standard deviations above the mean is chosen, its value will be 0.08. At the signal location, the mean and standard deviation are 0.38 and 0.14. Thus, the mean value at the signal location is slightly more than two standard deviations above the threshold level. A similar calculation for the high-resolution technique shows the signal mean to be about 1.8 standard deviations above the threshold.

In Figure II-1 (SNR = 0.72), both techniques result in signal means that are about 1.5 standard deviations above the threshold (two standard deviations above the noise mean at 0.04 cycle/km). It appears that the high-resolution scheme offers better detectability at low SNR's, while the converse is true for SNR's above about 0.7.

This tendency is also evinced in Figure II-3, where the abscissa measures SNR. Here, the standard deviations of the two schemes have fairly similar slopes, but the slope of the mean for the conventional spectrum is appreciably greater than that for the high-resolution spectrum. This is consistent with the superiority of the conventional spectrum at higher SNR's.

In summary, for an SNR of 1.0, it is possible to choose a threshold level which is two standard deviations above the mean level for uncorrelated ambient noise and two standard deviations below the mean level for the signal as seen by the conventional spectrum. While slightly inferior at this SNR, the high-resolution scheme apparently becomes somewhat superior for SNR values below 0.7.

Figure II-4 illustrates the performance of these processing schemes for locating a signal in uncorrelated ambient noise. An infinite-velocity signal was embedded in each of 100 independent random-noise vectors.

science services division

For each resultant signal-plus-noise vector, the conventional spectrum was evaluated at 25 equispaced locations between 0.0 and 0.096 cycle/km along the N-S axis, and the peak-power location was determined. For uncorrelated noise, these peak-power locations are necessarily the same as those resulting from the high-resolution schemes or from the probabilistic processor (described in Appendix A). Figure II-4 shows, for various SNR, the number of times out of 100 that the peak power occurs at each of these wavenumber locations. To add perspective, note that at 1.0 Hz the wavenumber space distance between 0.044 and 0.048 cycle/km corresponds to about 700-km separation between epicenters, while the distance between 0.068 and 0.072 cycle/km corresponds to about 625-km epicenter separation. Also note that the locations at which the spectrum is evaluated include the true signal locations but only a small fraction of the total number of other locations defined by a rectangular grid having a 0.004-cycle/km spacing between nearest locations. Thus, the results in Figure II-4 provide an upper bound on the relative fraction of correct locations that can be expected.

Subject to this limitation, it is seen that a large number of incorrect locations occur for an SNR of 0.25 or 0.50. At an SNR of 1.0, however, the signal was located properly 98 times out of 100.

When a velocity-preserving stack over five independent frequencies is formed, as described in Section II, subsection C, significantly better performance results. Figure II-5 shows that in this case, the 0.25 SNR still leads to a number of incorrect locations but for an SNR of 0.50 or 1.0, the signal is always located correctly. The data in Figure II-5 are appropriate only for the conventional spectrum technique. Stacking of the other types of spectra would lead to other — but probably similar — results,

implying that stacking over frequencies in the frequency domain is significantly superior to location at a single frequency. When stacking is done, it appears possible to properly locate the signal for an SNR greater than 0.50. It is likely that the analogous procedure of selecting the largest of a grid of time-domain beamsteers would lead to similar results.

Figures II-6, II-7, and II-8 illustrate the performance of a 25-element conventional subarray with a noise model that is largely correlated. The model consists of an isotropic disk, centered at the origin with a radius of 0.1 cycle/km, to which 20-percent uncorrelated noise has been added. In this case and all subsequent correlated noise cases, the procedure consists of generating the 100 signal-plus-noise vectors, calculating the conventional and high-resolution spectra at 11 equispaced points along the N-S axis for each of the vectors, normalizing the result for each vector so that the 11 values calculated sums to unity, and then calculating the mean and standard deviation over the 100 normalized sets of data.

Figure II-6 shows the means and standard deviations for conventional and high-resolution spectra as a function of wavenumber at an SNR of 0.0042. This small amount of signal has virtually no effect on the resultant spectra, so the results illustrate the appearance of noise alone. The results for an SNR of 0.6 (Figure II-7) shows that it is not possible to pick a threshold for either spectral technique that would almost always be above the noise peak and below the signal peak. Detection with a standard subarray in this type of highly correlated noise would be possible only for SNR's much greater than 0.6. The data in Figures II-6 and II-7 indicate that the high-resolution technique probably can detect smaller signals than can the conventional technique. This conclusion seems consistent with the data of Figure II-8, where the means and standard deviations are plotted as a function of SNR at the signal location, 0.0 cycle/km.

The noise model used for Figures II-9, JI-10, and II-11 consists
of a disk centered at 0.05 cycle/km on the N-S axis with 0.01-cycle/km
radius and 1-percent uncorrelated noise added. Figure II-9 shows the means
and standard deviations as a function of wavenumber, while Figures II-10
and II-11 show the means and standard deviations plotted vs SNR at 0.0 and
0.05 cycle/km, respectively. For the conventional spectrum, a threshold
at 0.12 is almost always above the largest noise peak. Such a threshold,
however, is above the mean value at the signal location for any of the SNR's
considered. An appropriate threshold for the high-resolution spectrum
would be about 0.095. At an SNR of 0.4, the threshold is below the mean at
the signal location, but the difference is less than one standard deviation. The
separation increases slightly with SNR but is still less than one standard
deviation at the largest SNR considered, 0.9. The conclusion apparently is
that for subarray processing with the noise field consisting of very concen-
trated bodywave noise, the conventional spectrum has questionable value for
detection, while the high-resolution technique has marginal value.

Shown in Figures II-12 through II-18 are means and standard
deviations resulting from a noise model comprising a disk with a 0.025-
cycle/km radius centered at 0.05 cycle/km on the N-S axis. Figures II-12
and II-13 result from noise models having 1-percent uncorrelated noise
added. Figures II-14, II-15, II-16, and II-17 have 10-percent uncorrelated
noise added to the noise model. Figure II-18 has 20-percent uncorrelated
noise added. This model represents bodywave noise which is mostly direc-
tional but fairly widespread. The array configuration consists of the center
and outer 15 locations of a standard LASA subarray.

Although not shown in these figures, the data for all three per-
centages of uncorrelated noise show that the largest peaks — when noise

alone is present — occur at 0.0-cycle/km wavenumber for both spectral techniques. Thus, from Figures II-13, II-17, and II-18, the means and standard deviations at the origins may be used to select appropriate threshold levels. If the threshold is chosen to be two standard deviations above the noise mean for the conventional spectrum, the resultant level is above the mean at the signal location for all SNR's considered. For the high-resolution technique, the resultant level is below the mean at the signal location for SNR's above 0.4; but in all cases, the difference is less than one standard deviation. The conclusion is the same as that for very concentrated bodywave noise: the conventional spectrum seemingly has little detection potential, while the high-resolution technique is marginal for SNR's above 0.4.

Location ability using the probabilistic processor is contrasted to that for the conventional and high-resolution spectral techniques in Figures II-19 and II-20. The center and outer 15 locations of a standard LASA subarray provided the 16 elements used, and 10-percent uncorrelated noise was added. For these figures, the processor outputs were calculated at 13 wavenumber locations with a 0.01-cycle/km separation. As before, the results obtained with the high-resolution spectrum are identical to those obtained with the conventional spectrum. The figures show that even for an SNR as high as 6.48, any of the spectral techniques applied to an array the size of a standard LASA subarray result in a fairly large number of incorrect locations.

APPENDIX A

DERIVATION OF PROCESSING EQUATIONS

BLANK PAGE

APPENDIX A
DERIVATION OF PROCESSING EQUATIONS

A. PROBABILISTIC PROCESSING EQUATION

Frequency-domain probabilistic processing is a method using seismic array data to detect plane-wave signals in the presence of ambient seismic noise. This method is based on the assumption that the array data is Gaussian with zero mean and known crosspower matrix $\left[Q_n\right]$ or $\left[Q_{s+n}^m\right]$ depending on the absence or presence of signal. The array output is considered to be k complex numbers resulting from the collateral Fourier transform of time gates from k channels of simultaneous array time-domain data.

The criteria for estimating the presence or the absence of a plane-wave signal is analogous to testing the simple hypothesis that the observed data have a crosspower matrix $\left[Q_n\right]$, with the alternate multiple hypotheses that the data are from a set of crosspower matrices of the form $\left[Q_{s+n}^m\right]$. The superscript m refers to a particular plane-wave signal model.

Derivation of the Gaussian multichannel sampled data processing equation starts with the multivariate Gaussian probability distribution.

$$P(x_1, x_2, \ldots, x_k) = \frac{1}{\pi^k \, |X|} \exp \left\{ - \{X\}_i^{*T} [X]^{-1} \{X\}_i \right\} \qquad (A-1)$$

In this equation, matrix notation is used as follows:

$\{X\}_i$ or X_i = i^{th} set of complex data values $x_1, x_2, \ldots, x_k$, with x_1 being the Fourier transform of the first time gate

$[X]$ or X = crosspower matrix of the data; i.e., $X_{ij} = X_i^* X_j$

The superscript T designates the matrix transpose; the superscript -1 desig-
nates the inverse matrix; and the superscript * signifies the matrix complex
conjugate. Vertical lines bordering a square matrix indicate the matrix
determinant.

In Equation A-1, k is the number of data values. In a multi-
channel problem, k would usually be equal to the number of channels.

The detection of a plane-wave signal in the presence of ambient
seismic noise can be formulated as a multipossibility multichannel Gaussian
problem. That is, one can assume that the data X_i is a sample of a stationary
Gaussian time series have a k by k crosspower matrix composed of noise
$\left[Q_n\right]$ or one of a set of signal-plus-noise matrices $\left[Q_{s+n}^m\right]$.

To completely specify the problem using a Bayesian approach,
the a priori probabilities $P(Q_n)$, $P\left(Q_{s+n}^m\right)$ of the possibilities must be known
or estimated. The problem is to obtain the a posteriori probabilities of noise
alone $P(Q_n | X_i)$ and of signal plus noise $P(Q_{s+n}^m | X_i)$ by analyzing the data X_i.
It is understood that $\left[Q_{s+n}^m\right]$ ranges over all allowable plane-wave signal
models.

In the seismic detection problem, Q_n stands for ambient
seismic noise and $P(Q_n)$ is the fraction of time that no signal is present.
Q_{s+n}^m stands for a particular signal model in the presence of noise, and
$P(Q_{s+n}^m)$ is the fraction of time that this signal is present.

A statement of the a posteriori probability using Bayes theorem
for noise alone is

$$P(Q_n | X_i) = \frac{P(X_i | Q_n)}{P(X_i)} \; P(Q_n) \qquad (A-2)$$

For signal plus noise, the a posteriori probability is

$$P(Q^m_{s+n} \mid X_i) = \frac{P(X_i \mid Q^m_{s+n})}{P(X_i)} \; P(Q^m_{s+n}) \tag{A-3}$$

From Equation A-1,

$$P(X_i \mid Q_n) = \frac{1}{\pi^k \mid Qn \mid} \; \exp \left\{ -X_i^{*T} \left[Q_n \right]^{-1} X_i \right\} \tag{A-4}$$

and

$$P(X_i \mid Q^m_{s+n}) = \frac{1}{\pi^k \mid Q^m_{s+n} \mid} \; \exp \left\{ -X_i^{*T} \left[Q^m_{s+n} \right]^{-1} X_i \right\} \tag{A-5}$$

with

$$P(X_i) = \frac{P(Q_n)}{\pi^k \mid Q_n \mid} \; \exp \left\{ -X_i^{*T} \left[Q_n \right]^{-1} X_i \right\} \tag{A-6}$$

$$+ \sum_m \frac{P(Q^m_{s+n})}{\pi^k \mid Q^m_{s+n} \mid} \; \exp \left\{ -X_i^{*T} \left[Q^m_{s+n} \right]^{-1} X_i \right\} \tag{A-7}$$

From these equations, the a posteriori probabilities are

$$P(Q_n \mid X_i) = \frac{\dfrac{P(Q_n)}{\pi^k \mid Q_n \mid} \; \exp \left\{ -X_i^{*T} \left[Q_n \right]^{-1} X_i \right\}}{P(X_i)} \tag{A-8}$$

and

$$P(Q_{s+n}^m \mid X_i) = \cfrac{\cfrac{P(Q_{s+n}^m)}{\pi^k \mid Q_{s+n}^m \mid} \exp\left\{-X_i^{*T} \left[Q_{s+n}^m\right]^{-1} X_i\right\}}{P(X_i)} \tag{A-9}$$

The denominator of Equations A-8 and A-9 normalizes $P(Q_n \mid X_i)$ and $P(Q_{s+n}^m \mid X_i)$ so that their sum is 1. Equation A-9 may be normalized by replacing the denominator in Equation A-9 by the summation of the numerator over the possible values of m. In this case, the possibility that no signal is present is removed. Furthermore, if it is assumed that the probabilities of the occurrence of the various signals is equally likely, Equation A-9 becomes

$$P(Q_{s+n}^m \mid X_i) = \cfrac{\cfrac{1}{\mid Q_{s+n}^m \mid} \exp\left\{-X_i^{*T} \left[Q_{s+n}^m\right]^{-1} X_i\right\}}{\displaystyle\sum_m \cfrac{1}{\mid Q_{s+n}^m \mid} \exp\left\{-X_i^{*T} \left[Q_{s+n}^m\right]^{-1} X_i\right\}} \tag{A-10}$$

For locating a plane-wave in noise, the crosspower matrix becomes

$$\left[Q_{s+n}^m\right] = \left[N + VV^{*T}\right]$$

where N is the noise crosspower matrix and

$$V = \left\{ \begin{array}{c} e^{i\vec{k} \cdot \vec{r}_1} \\ e^{i\vec{k} \cdot \vec{r}_2} \\ . \\ . \\ . \\ e^{i\vec{k} \cdot \vec{r}_k} \end{array} \right\}$$

science services division

with

$\vec{k}$ = vector wavenumber

$\vec{r}_p$ = p^{th} array coordinate corresponding to the pth data channel

Thus, the superscript m denotes a plane-wave signal located at one of the possible points in K-space.

For computational purposes the inverse of the crosspower matrix may be written as*

$$\left[N + V V^{*T}\right]^{-1} = N^{-1} - \frac{N^{-1} V V^{*T} N^{-1}}{1 + V^{*T} N^{-1} V} \qquad (A-11)$$

B. HIGH-RESOLUTION FREQUENCY-WAVENUMBER SPECTRA

High-resolution frequency-wavenumber spectra are computed from a frequency-domain multichannel filter. In the filter synthesis, the signal crosspower matrix is assumed to be uncorrelated Gaussian noise, and the noise crosspower matrix is measured data.

The multichannel filter designed at a single frequency is

$$\left[WI + X_i X_i^{*T}\right] F_n^* = \Gamma_n \qquad (A-12)$$

_____

*The formula used is $(A + XY^{*T})^{-1} = R - RX(1 + X^{*T}RY)^{-1} Y^{*T}R$, where X and Y are row matrices (vectors) and $R = A^{-1}$. Both A and $(A + XY^{*T})$ are assumed to be nonsingular.

where

$$
F_n^* = \begin{Bmatrix} f_1 \\ f_2 \\ \cdot \\ \cdot \\ \cdot \\ f_k \end{Bmatrix} \qquad\qquad \Gamma_n = \begin{Bmatrix} 0 \\ \cdot \\ \cdot \\ w \\ \cdot \\ \cdot \\ 0 \end{Bmatrix}
$$

k and X_i are defined in the previous sections; w is a scale factor; and I is the identity matrix. The subscript n ($1 \le n \le k$) specifies the reference channel used in the filter design.

Using the nth channel as reference, the solution to Equation A-12 is

$$
F_n^* = \frac{1}{w} \left[I - \frac{1}{(w + X_i^{*T} X_i)} X_i X_i^{*T} \right] \Gamma_n \tag{A-13}
$$

A high-resolution frequency-wavenumber spectra may be computed from Equation A-13 with a single sensor as reference, or

$$
V^T F_n^* F_n^T V^* \tag{A-14}
$$

Summation of the responses from using each channel as reference results in

$$
\sum_n V^T F_n^* F_n^T V^* = V^T \left[\sum_n F_n^* F_n^T \right] V^* \tag{A-15}
$$

A-6

Letting $B_n = \frac{1}{N} \Gamma_n$. Equation A-14 becomes

$$\sum_n v^T F_n^* F_n^T v^* = v^T \left[\sum_n B_n^* B_n^T \right] v^* \qquad \text{(A-16)}$$

$$- \frac{2}{w + X_i^{*T} X_i} v^T \left[\sum_n B_n^* B_n^T \right] X_i X_i^{*T} v^*$$

$$+ \frac{1}{(w + X_i^{*T} X_i)^2} v^T X_i X_i^{*T} \left[\sum_n B_n^* B_n^T \right] X_i X_i^{*T} v^*$$

However, when all sensors are used as reference,

$$\sum_n B_n^* B_n^T = I \qquad \text{(A-17)}$$

and Equation A-16 simplifies to

$$v^T v^* - (v^T X_i^*)(v^T X_i^*)^* \frac{(2w + X_i^{*T} X_i)}{(w + X_i^{*T} X_i)^2}$$

APPENDIX B

DETERMINANT EVALUATION

APPENDIX B
DETERMINANT EVALUATION

It is desired to develop an efficient method for the evaluation of $|N + VV^{*T}|$ for a large number of values of $\vec{k}$. Here, N is a covariance matrix and $V = V(\vec{k})$ is a unit plane-wave transform for a signal at the vector $\vec{k}$ in wavenumber space.

First, the following theorem is proven. Let I_n denote the $(n \times n)$ identity matrix and $W_n^T = (w_1, w_2, \ldots w_n)$ denote an n-dimensional complex vector. Then,

$$|I_n + W_n W_n^{*T}| = 1 + W_n^{*T} W_n$$

This is proved by induction on the integer n.

Clearly the theorem holds for $n = 1$. Assume that it holds for $n = r$. The problem is to show that the theorem holds for $n = r + 1$. Let

$$|Z_r| = \left[I_r + W_r W_r^{*T}\right]$$

Partition Z_{r+1} such that

$$\left[Z_{r+1}\right] = \left[\begin{array}{c|c} Z_r & M \\ \hline M^{*T} & 1 + w_{r+1} w_{r+1}^* \end{array}\right]$$

where

$$M^T = (w_1 w_{r+1}^*, \ldots, w_r w_{r+1}^*)$$

Let $\alpha = 1 + w_{r+1} w_{r+1}^*$. Then $|Z_{r+1}|$ can be written as

science services division

$$|Z_{r+1}| = |Z_r - M\alpha^{-1}M^{*T}| \cdot |\alpha|$$

But

$$\left[Z_r - M^{-1}M^{*T}\right] = \left[I_r + \alpha^{-1}W_r W_r^{*T}\right]$$

which may be verified by direct computation. Then by assumption,

$$|Z_{r+1}| = |I_r + \alpha^{-1}W_r W_r^{*T}| \cdot |\alpha|$$

$$= (1 + \alpha^{-1}W_r^{*T}W_r)\alpha$$

Thus,

$$|Z_{r+1}| = \alpha + W_r^{*T}W_r$$

$$= 1 + w_{r+1}w_{r+1}^* + W_r^{*T}W_r$$

$$= 1 + W_{r+1}^{*T}W_{r+1}$$

Q. E. D.

To evaluate $|N + VV^{*T}|$, consider

$$N + VV^{*T}$$

Since N is positive definite Hermitian, there exists a matrix S such that

$$SNS^{*T} = I$$

It follows that

$$S(N+VV^{*T})S^{*T} = SNS^{*T} + SVV^{*T}S^{*T} = I + WW^{*T}$$

science services division

where $W = SV$. Then

$$\left| S(N + VV^{*T}) S^{*T} \right| = \left| S \right| \left| N + VV^{*T} \right| \left| S^{*T} \right| = \left| I + WW^{*T} \right|$$

Making use of the previously proven theorem, this becomes

$$\left| N + VV^{*T} \right| = \left| N \right| (1 + W^{*T} W)$$

which is an efficient method for evaluating $\left| N + VV^{*T} \right|$.

DOCUMENT CONTROL DATA - R&D

(Security classification of title, body of abstract and indexing annotation must be entered when the overall report is classified)

1. ORIGINATING ACTIVITY (Corporate author)	2a. REPORT SECURITY CLASSIFICATION
Texas Instruments Incorporated	Unclassified
Science Services Division	2b. GROUP
P. O. Box 5621, Dallas, Texas 75222	

3. REPORT TITLE

LOCATION STATISTICS FOR FREQUENCY-WAVENUMBER PROCESSING — LARGE-ARRAY SIGNAL AND NOISE ANALYSIS SPECIAL SCIENTIFIC REPORT NO. 25

4. DESCRIPTIVE NOTES (Type of report and inclusive dates)

Special Scientific

5. AUTHOR(S) (Last name, first name, initial)

Wilkins, Wayne W.
Heiting, Leo N.

6. REPORT DATE	7a. TOTAL NO. OF PAGES	7b. NO. OF REFS
21 November 1968	51	0

8a. CONTRACT OR GRANT NO.	9a. ORIGINATOR'S REPORT NUMBER(S)
Contract No. AF 33(657)-16678	
b. PROJECT NO.	
Project No. VT/6707	
c.	9b. OTHER REPORT NO(S) (Any other numbers that may be assigned this report)
d.	

10. AVAILABILITY/LIMITATION NOTICES

This document is subject to special export control and each transmittal to foreign governments or foreign nationals may be made only with prior approval of Chief, AFTAC.

11. SUPPLEMENTARY NOTES	12. SPONSORING MILITARY ACTIVITY
ARPA Order No. 599	Air Force Technical Applications Center
	VELA Seismological Center
	Headquarters, USAF, Washington, D. C.

13. ABSTRACT

Results of a computer study which theoretically determined the detection and location capabilities of various wavenumber spectral techniques are presented in this report. Two distinct short-period array configurations were simulated. The first configuration simulated was a 13-element array employing the outputs of the inner 13 subarrays of the Montana LASA. In this case, the ambient noise was considered to be completely uncorrelated. The second configuration simulated consisted of all or a portion of a standard LASA subarray. Various noise models, made up of mostly organized noise, were used. Four spectral techniques — the conventional spectrum, two high-resolution spectra, and the probabilistic processor — were evaluated. When wavenumber spectra at a single frequency are used to locate a signal in uncorrelated noise, all four techniques must yield exactly the same location. It was found that events with a SNR of 1.0 or greater were almost always located properly within the resolving power of the grid points at which the spectra were calculated. Wideband frequency-domain location can be accomplished by computing wavenumber spectra at several independent frequencies and summing the spectra in a velocity-preserving manner before choosing the peak-power location. Conventional spectra of signals in uncorrelated noise were computed at five independent frequencies and summed. This procedure results in no incorrect locations for SNR's of 0.5 or greater, thereby indicating its significant superiority over the location ability of single-frequency spectra. The wideband wavenumber spectral technique is roughly analogous to time-domain beamforming, and the results obtained here may be indicative of those achievable in the time domain. The performance of the small arrays in organized noise was found to be markedly inferior to the performance of the large array using uncorrelated noise. The conventional spectrum seems to have no practical detection ability, while the high-resolution techniques are perhaps marginal in this respect. All techniques located a significant number of events improperly, even when the SNR was as high as 6.48.

DD FORM 1473
1 JAN 54

14. KEY WORDS	LINK A		LINK B		LINK C	
	ROLE	WT	ROLE	WT	ROLE	WT
Large-Array Signal and Noise Analysis						
LASA Array						
Location Statistics						
Frequency-Wavenumber Processing						
Detection Capabilities						
Short-Period Arrays						
Conventional Spectrum						
High-Resolution Spectra						
Propabilistic Processor						

INSTRUCTIONS

1. **ORIGINATING ACTIVITY:** Enter the name and address of the contractor, subcontractor, grantee, Department of Defense activity or other organization (*corporate author*) issuing the report.

2a. **REPORT SECURITY CLASSIFICATION:** Enter the overall security classification of the report. Indicate whether "Restricted Data" is included. Marking is to be in accordance with appropriate security regulations.

2b. **GROUP:** Automatic downgrading is specified in DoD Directive 5200.10 and Armed Forces Industrial Manual. Enter the group number. Also, when applicable, show that optional markings have been used for Group 3 and Group 4 as authorized.

3. **REPORT TITLE:** Enter the complete report title in all capital letters. Titles in all cases should be unclassified. If a meaningful title cannot be selected without classification, show title classification in all capitals in parenthesis immediately following the title.

4. **DESCRIPTIVE NOTES:** If appropriate, enter the type of report, e.g., interim, progress, summary, annual, or final. Give the inclusive dates when a specific reporting period is covered.

5. **AUTHOR(S):** Enter the name(s) of author(s) as shown on or in the report. Enter last name, first name, middle initial. If military, show rank and branch of service. The name of the principal author is an absolute minimum requirement.

6. **REPORT DATE:** Enter the date of the report as day, month, year; or month, year. If more than one date appears on the report, use date of publication.

7a. **TOTAL NUMBER OF PAGES:** The total page count should follow normal pagination procedures, i.e., enter the number of pages containing information.

7b. **NUMBER OF REFERENCES:** Enter the total number of references cited in the report.

8a. **CONTRACT OR GRANT NUMBER:** If appropriate, enter the applicable number of the contract or grant under which the report was written.

8b, 8c, & 8d. **PROJECT NUMBER:** Enter the appropriate military department identification, such as project number, subproject number, system numbers, task number, etc.

9a. **ORIGINATOR'S REPORT NUMBER(S):** Enter the official report number by which the document will be identified and controlled by the originating activity. This number must be unique to this report.

9b. **OTHER REPORT NUMBER(S):** If the report has been assigned any other report numbers (*either by the originator or by the sponsor*), also enter this number(s).

10. **AVAILABILITY/LIMITATION NOTICES:** Enter any limitations on further dissemination of the report, other than those imposed by security classification, using standard statements such as:

(1) "Qualified requesters may obtain copies of this report from DDC."

(2) "Foreign announcement and dissemination of this report by DDC is not authorized."

(3) "U. S. Government agencies may obtain copies of this report directly from DDC. Other qualified DDC users shall request through

_____."

(4) "U. S. military agencies may obtain copies of this report directly from DDC. Other qualified users shall request through

_____."

(5) "All distribution of this report is controlled. Qualified DDC users shall request through

_____."

If the report has been furnished to the Office of Technical Services, Department of Commerce, for sale to the public, indicate this fact and enter the price, if known.

11. **SUPPLEMENTARY NOTES:** Use for additional explanatory notes.

12. **SPONSORING MILITARY ACTIVITY:** Enter the name of the departmental project office or laboratory sponsoring (*paying for*) the research and development. Include address.

13. **ABSTRACT:** Enter an abstract giving a brief and factual summary of the document indicative of the report, even though it may also appear elsewhere in the body of the technical report. If additional space is required, a continuation sheet shall be attached.

It is highly desirable that the abstract of classified reports be unclassified. Each paragraph of the abstract shall end with an indication of the military security classification of the information in the paragraph, represented as *(TS)*, *(S)*, *(C)*, or *(U)*.

There is no limitation on the length of the abstract. However, the suggested length is from 150 to 225 words.

14. **KEY WORDS:** Key words are technically meaningful terms or short phrases that characterize a report and may be used as index entries for cataloging the report. Key words must be selected so that no security classification is required. Identifiers, such as equipment model designation, trade name, military project code name, geographic location, may be used as key words but will be followed by an indication of technical context. The assignment of links, rules, and weights is optional.

GPO 886-551